issn 0065-3713

INSTITUT D'AERONOMIE SPATIALE DE BELGIQUE

3 - Avenue Circulaire
B - 1180 BRUXELLES

AERONOMICA ACTA

A - N° 331 - 1988

Aeronomic problems of molecular oxygen photodissociation - II. Theoretical absorption cross-sections of the Schumann-Runge bands at 79 K

by

Marcel NICOLET, Stanislas CIESLIK

and Robert KENNES

BELGISCH INSTITUUT VOOR RUIMTE-AERONOMIE

3 - Ringlaan
B - 1180 BRUSSEL

FOREWORD

Aeronomic problems of molecular oxygen photodissociation - II. "Theoretical absorption cross sections of the Schumann-Runge bands at 79 K" will be published in Planetary Space Science, volume 36, 1988.

AVANT-PROPOS

Aeronomic problems of molecular oxygen photodissociaton - II. "Theoretical absorption cross sections of the Schumann-Runge bands at 79 K" sera publié dans Planetary Space Science, volume 36, 1988.

VOORWOORD

Aeronomic problems of molecular oxygen photodissociation - II. "Theoretical absorption cross sections of the Schumann-Runge bands at 79 K" zal gepubliceerd worden in Planetary Space Science, boekdeel 36, 1988.

VORWORT

Aeronomic problems of molecular oxygen photodissociation - II. "Theoretical absorption cross sections of the Schumann-Runge bands at 79 K" wird publiziert werden in Planetary Space Science, Volumen 36, 1988.

AERONOMIC PROBLEMS OF MOLECULAR OXYGEN PHOTODISSOCIATION - II. THEORETICAL ABSORPTION CROSS SECTIONS OF THE SCHUMANN-RUNGE BANDS AT 79 K

by

Marcel NICOLET*, Stanislas CIESLIK** and Robert KENNES

Institut d'Aéronomie Spatiale de Belgique
3, Avenue Circulaire, B-1180 BRUSSELS, Belgium

Abstract

Theoretical spectra corresponding to the domain of the rotational lines of the 2-0 to 12-0 bands of the $B\ ^3\Sigma_u^- - X\ ^3\Sigma_g^-$ Schumann-Runge system of O_2 at 79 K are presented in graphical format. Calculated absorption cross sections are compared with recent laboratory measurements made at the same temperature. The calculations were based on previous theoretical determinations at 300 K established after a comparison with results of laboratory measurements made at the same temperature. Such an analysis in which the band oscillator strengths are associated with averaged line-widths of the rotation lines for each band and with their underlying continuum, gives consistent values for the various spectroscopic parameters of the O_2 Schumann-Runge bands.

Résumé

Les spectres théoriques correspondant au domaine des raies de rotation des bandes 2-0 à 12-0 du système Schumann-Runge $B\ ^3\Sigma_u^- - X\ ^3\Sigma_g^-$ de O_2 à 79 K sont représentés par une série de figures. Les sections efficaces d'absorption calculées sont comparées avec celles résultant des mesures de laboratoires récemment effectuées à la même température. Les calculs ont été basés sur des déterminations théoriques antérieures à 300 K établies après une comparaison avec des résultats de mesures de laboratoire effectuées à la même température. Une telle analyse, dans laquelle les forces d'oscillateur sont associées avec les largeurs moyennes des raies de rotation pour chaque bande et avec le continuum adjacent, conduit à des valeurs compatibles pour l'ensemble des paramètres spectroscopiques des bandes Schumann-Runge de O_2.

---

* : Also with : Communications and Space Sciences Laboratory, Penn State University, University Park, PA 16802.

** : Now at : Commission of the European Communities, ISPRA Establishment, Italy, Chemistry Division, Air Pollution Sector.

Samenvatting

De theoretische spectra die overeenstemmen met het domein der rotatielijnen van de banden 2-0 tot 12-0 van het Schumann-Runge systeem $B\ ^3\Sigma_u^- - X\ ^3\Sigma_g^-$ van O_2 bij 79 K, worden door een reeks figuren voorgesteld. De berekende werkzame absorptiedoorsneden worden vergeleken met recente laboratoriummetingen die bij dezelfde temperatuur uitgevoerd werden. De berekeningen steunden op vorige theoretische bepalingen bij 300 K, opgesteld na vergelijking met de resultaten van laboratoriummetingen verricht bij dezelfde temperatuur. Een dergelijke analyse, waarin de oscillatorkrachten verbonden zijn met de gemiddelde breedten van de rotatielijnen voor iedere band en met het aangrenzend continuum, leidt tot overeenstemmende waarden voor het geheel van de spectroscopische parameters van de Schumann-Runge banden van O_2.

Zusammenfassung

Die theoretischen Spektren im Gebiet des Rotationslinien der Banden 2-0 bis 12-0 des O_2 Schumann-Runge Systems $B\ ^3\Sigma_u^- - X\ ^3\Sigma_g^-$ um 79 K werden durch eine Reihenfolge von Figuren dargestellt. Die berechneten Absorptionsquerschnitten werden verglichen mit Laboratoriumsmessungen kürzlich ausgeführt an der gleichen Temperatur. Die Berechnungen wurden auf früheren theoretischen Bestimmungen bei 300 K begründet, nach einem Vergleich mit Ergebnissen von Laboratoriumsmessüngen ausgeführt an der gleichen Temperatur. Eine solche Analyse, in welcher die Oszillatorkräfte mit den mittleren Breiten der Rotationslinien jedes Bandes und mit dem anliegenden Kontinuum verbunden werden, leitet zu konsistenten Werten für die gesamten spektroskopischen Parametern der O_2 Schumann-Runge Banden.

I. INTRODUCTION

In a recent publication (Nicolet et al., 1987) a theoretical determination of the rotational structure and absorption cross sections of the O_2 Schumann-Runge bands (see Table 1) was made at 300 K. This detailed analysis was based on the experimental results obtained by the Harvard - Smithsonian Group on the photodissociation absorption cross sections at high resolution in the spectral region corresponding to the v' = 1 to 12 bands (Yoshino et al., 1983).

After the first detailed analyses such as the wavelength assignments, for $v' \geq 12$, of Brix and Herzberg (1954) and, for $v' \leq 13$, of Ackerman and Biaumé (1970) and Biaumé (1972), extensive wavenumber measurements of the rotation lines of the O_2 Schuman-Runge absorption bands were provided by Yoshino et al., (1984). These sets of data are also the most accurate and most complete since the cross sections are absolute, the linewidths being in excess of the instrument resolution for the various bands studied.

Recent rotational constants (Table 2) of the upper electronic state of the Schumann-Runge system have also been published by Cheung et al. (1986). These constants make it possible to calculate the wavenumbers of the rotation lines. The same spectroscopic constants have been also determined by Lewis et al., (1986) from the wavenumber measurements of Yoshino et al., (1984).

The adopted band oscillator strengths of the (v', 0) and (v', 1) bands were based on the various results of Yoshino et al., (1983), of Cheung et al. (1986), and of Lewis et al. (1986b).

The mean predissociation linewidths were determined after a detailed comparison between calculated absorption cross sections and the experimental results published by Yoshino et al. (1983) in the spectral region corresponding to the v' = 1 to 12 bands. However, the absorption

TABLE 1.- Adopted spectral intervals for the Schumann-Runge bands of O_2

Band	Wavenumber (cm^{-1})	Mean	$\Delta\nu$	Wavelength (nm)	Mean	$\Delta\lambda$
0-0	49000-49500	49250	500	204.08-202.02	203.04	2.06
1-0	49500-50050	49777	550	202.02-199.80	200.90	2.22
2-0	50050-50715	50382	665	199.80-197.18	198.48	2.62
3-0	50715-51355	51035	640	197.18-194.72	195.94	2.46
4-0	51355-51975	51665	620	194.72-192.40	193.55	2.32
5-0	51975-52565	52270	590	192.40-190.24	191.31	2.16
6-0	52565-53130	52847	565	190.24-188.22	189.22	2.02
7-0	53130-53660	53395	530	188.22-186.36	187.28	1.86
8-0	53660-54160	53910	500	186.36-184.64	185.49	1.72
9-0	54160-54625	54392	465	184.64-183.07	183.85	1.57
10-0	54625-55055	54840	430	183.07-181.64	182.35	1.43
11-0	55055-55440	55247	385	181.64-180.37	181.00	1.27
12-0	55440-55790	55615	350	180.37-179.14	179.80	1.13
13-0	55790-56090	55940	300	179.24-178.28	178.76	0.96
14-0	56090-56345	56217	255	178.28-177.48	177.88	0.80
15-0	56345-56550	56447	205	177.48-176.83	177.16	0.65
16-0	56550-56725	56637	175	176.83-176.29	176.56	0.57
17-0	56725-56855	56790	130	176.29-175.89	176.09	0.40
18-0	56855-56960	56907	105	175.89-175.56	175.72	0.33
19-0	56960-57035	56997	75	175.56-175.33	175.45	0.23

TABLE 2.- Adopted spectroscopic constants for the upper state of the Schumann-Runge bands of O_2 to compute line positions.

Band	$\nu_o(cm^{-1})$	B_v	D_v	λ_v	γ_v
0-0	49357.96	0.8132	4.50×10^{-6}	1.69	$-2.80.x.10^{-2}$
1-0	50045.53	0.7993	4.20	1.70	- 2.60
2-0	50710.68	0.7860	5.80	1.69	- 2.90
3-0	51351.94	0.7705	5.20	1.70	- 2.60
4-0	51969.36	0.7550	5.97	1.81	- 3.00
5-0	52560.94	0.7377	5.80	1.75	- 2.20
6-0	53122.65	0.7187	5.00	1.79	- 2.10
7-0	53655.95	0.7010	8.60	1.82	- 2.10
8-0	54156.22	0.6770	6.70	1.91	- 2.30
9-0	54622.50	0.6514	6.30	2.04	- 2.10
10-0	55051.16	0.6263	9.90	2.10	- 4.10
11-0	55439.23	0.5956	9.40	2.17	- 3.80
12-0	55784.58	0.5626	1.37×10^{-5}	2.37	- 5.40
13-0	56085.44	0.5242	1.63	2.51	- 8.40
14-0	56340.42	0.4832	2.09	2.81	-1.16×10^{-1}
15-0	56550.62	0.4391	2.54	3.30	- 1.64
16-0	56719.62	0.3934	3.08	4.11	- 2.41
17-0	56852.45	0.3457	3.34	5.18	- 3.48
18-0	56951.60	0.2872	5.50	6.51	- 4.94
19-0	57025.80	0.2649	6.00	7.63	- 6.04

ν_o = band origin = $T + \frac{2}{3}\lambda - \gamma$ as given by Cheung et al. (1986)
B_v and D_v = rotational constants for vibrational levels
λ_v and γ_v splitting constants for vibrational levels.
For 18-0 and 19-0, see Fang, Wofsy and Dalgarno (1974).

cross sections throughout this region may depend also on the underlying continuum corresponding near 50000 cm^{-1} to the O_2 Herzberg continuum (see Nicolet and Kennes, 1986, and 1988). At wavenumbers greater than 55000 cm^{-1}, the O_2 Schumann-Runge continuum (see Lewis et al. 1985a, b) plays a role related to the temperature.

The recent extensive determination by Yoshino et al. (1987) of the experimental structure of the 2-0 to 12-0 bands at 79 K provides a direct test for the theoretical determination which must be used for aeronomic purposes (Temperatures generally between 170 and 270 K). In the present paper experimental data and theoretical results at 79 K are compared to provide an improved understanding of the absorption structure in the predissociation region of the O_2 Schumann-Runge system.

2. THE DAND OSCILLATOR STRENGTHS

The Schumann-Runge bands analyzed many times have generated several determinations of their mean oscillator strengths. The values adopted here (Table 3) are based mainly on the recent results of the Cambridge and Canberra groups to generate a consistent set of data (Yoshino et al., 1983; Cheung et al., 1984; Yoshino et al., 1987; Lewis et al. 1986) and also on the analysis of Allison et al. (1971). Since it is practically impossible to introduce an exact oscillator strength adapted to all circumstances, mean values have been adopted for each vibrational level. The uncertainties should be generally less than 5% but could reach perhaps 5 to 10% for 2 or 3 bands. In any case, the values given in Table 3 must be considered as averaged band oscillator strengths to be adopted in order to determine the effective linewidths of the rotational lines of bands corresponding to the various vibrational levels from $v' = 0$ to $v' = 19$.

3. ROTATIONAL PREDISSOCIATION LINEWIDTHS

The measured high resolution absorption cross sections of the Schumann-Runge bands by Yoshino et al. (1983) between 201 nm and 179 nm

TABLE 3.- Adopted mean absorption oscillator strengths $f_{v''v'}$ for the Schumann-Runge bands of O_2 deduced from absorption spectra.

v'	$f_{ov'}$	$f_{1v'}$
0	2.8×10^{-10}	7.6×10^{-9}
1	3.0×10^{-9}	8.2×10^{-8}
2	1.9×10^{-8}	4.6×10^{-7}
3	8.2×10^{-8}	1.8×10^{-6}
4	2.7×10^{-7}	5.0×10^{-6}
5	7.4×10^{-7}	1.3×10^{-5}
6	1.6×10^{-6}	2.7×10^{-5}
7	3.4×10^{-6}	5.0×10^{-5}
8	6.2×10^{-6}	8.6×10^{-5}
9	1.0×10^{-5}	1.2×10^{-4}
10	1.5×10^{-5}	1.7×10^{-4}
11	1.9×10^{-5}	2.1×10^{-4}
12	2.4×10^{-5}	2.6×10^{-4}
13	2.7×10^{-5}	2.6×10^{-4}
14	2.8×10^{-5}	2.9×10^{-4}
15	2.7×10^{-5}	2.7×10^{-4}
16	2.6×10^{-5}	2.0×10^{-4}
17	2.2×10^{-5}	1.6×10^{-4}
18	1.7×10^{-5}	1.3×10^{-4}
19	1.3×10^{-5}	1.6×10^{-4}

have been adopted to determine the effective rotational linewidths. Even when experimental results may have exhibited systematic variations with rotational levels (Lewis et al., 1986) an equivalent band linewidth was adjusted to fit the experimental absolute cross ssections after the introduction of the effect of an underlying continuum.

The Herzberg continuum plays an important role in the determination of an absorption cross sections of the first Schumann-Runge bands. The Schumann-Runge continuum is subject to a variation related to the population of the rotational and vibrational levels in the spectral range of the last bands near the normal continuum limit.

The best-fit model calculated values of the O_2 absorption cross sections with the experimental measurements have been used to determine the rotational linewidths adapted to each band. The adopted mean rotational linewidths are given in Table 4. The computation was made at each 0.1 cm^{-1} with a contributing spectral range of 500 cm^{-1} for a Voigt profile. Since realistic high resolution synthetic spectra require line centers to be located to within about 0.1 cm^{-1}, the wavenumbers obtained at each 0.1 cm^{-1} between 49000 cm^{-1} and 57000 cm^{-1} give the possibility of determining the detailed structure of the whole spectrum and of studying the effect of temperature. In addition, the relative role of the underlying continua with their related accuracy can be investigated as a function of temperature and wavelength.

4. THE O_2 HERZBERG CONTINUUM

The absorption cross sections of the O_2 Herzberg continuum at wavelengths greater than 200 nm used before 1980 must be now replaced by experimental and observational results obtained recently (1984 - 1986). An analysis made by Nicolet and Kennes (1986, and 1988) leads to the adoption of an empirical formula for the absorption cross section, $\sigma_{HERR}(O_2)$ cm^2,

$$\sigma_{HERR}(O_2) = 7.5 \times 10^{-24} (\nu/5 \times 10^4) \exp \{-50 [\ln(\nu/(5 \times 10^4)]^2\} \text{ cm}^{-1}$$

Although the available sets of Herzberg continuum cross sections derived from laboratory measurements seem to reach an acceptable agreement with their experimental accuracy at wavelengths greater than 200 nm, the errors of the experimental or theoretical determinations prevent an exact extrapolation for the Herzberg continuum underlying the Schumann-Runge bands between 190 and 200 nm. Nevertheless, the stratospheric determinations are not in disagreement with the values deduced from the formula that we have adopted.

Since our final determinations of the oxygen transmittance and of the photodissociation rate constants are given for spectral intervals of 500 cm^{-1}, mean absorption cross sections of the O_2 Herzberg continuum are used in our computations. The adopted numerical values are given in table 5.

5. ANALYSIS OF THE PHOTOABSORPTION CROSS SECTIONS

In our general analysis (Nicolet et al., 1987) the line positions and rotational assigments are reproduced for intervals of 250 cm^{-1} and the theoretical and experimental absorption cross sections are presented graphically (1 cm^{-1} per mm) at 300 K throughout the 49000 - 57000 cm^{-1} wavenumber region corresponding to all bands with v' = 0 to 19 and v" = 0 and 1. This graphical comparison between the calculated and measured absorption cross sections begins at 49750 cm^{-1}, 1 - 0 and 3-1 bands, and ends at 55800 cm^{-1}, 12-0 and 19-1 bands.

In order to show the principal features of the spectrum, 3 different regions (Rotational lines with their identifications in tables 6, 7 and 8) are illustrated in various figures by a semi-logarithmic plot of the absorption cross sections, namely between 50500 and 50750 cm^{-1} (Fig. 1a), 51750 and 52000 cm^{-1} (Fig. 2a), and 54000 and 54250 cm^{-1} (Fig. 3a). Such figures (Fig. 1a, 2a and 3a) make it possible to perform a detailed

TABLE 4.- Adopted mean rotation linewidths for the Schumann-Runge bands of O_2.

v'	cm^{-1}	v'	cm^{-1}
0	0.1	10	1.0
1	0.9	11	1.4
2	0.6	12	0.8
3	1.8	13	0.5
4	3.6	14	0.5
5	2.0	15	0.5
6	1.8	16	0.5
7	1.9	17	0.5
8	2.1	18	0.3
9	1.2	19	0.3

TABLE 5.- Mean absorption cross sctions of the O_2 Herzberg continuum deduced from formula (1).

Interval (cm^{-1})	Cross sections (cm^2)	Interval (cm^{-1})	Cross sections (cm^2)
49000-49500	7.2×10^{-24}	52000-52500	7.2×10^{-24}
49500-50000	7.4	52500-53000	7.0
50000-50500	7.5	53000-53500	6.7
50500-51000	7.5	53500-54000	6.4
51000-51500	7.5	54000-54500	6.0
51500-52000	7.4	54500-55000	5.6

TABLE 6.- Identification of O_2 Schumann-Runge rotational lines 50500-50750 cm^{-1}.

TABLE 6

IDENTIFICATION OF O_2 SCHUMANN-RUNGE ROTATIONNAL LINES 50500 - 50750 cm^{-1}

ν	λ	band	ν	λ	band
50500					
50522.9	1979.30	5-1 P25	50663.3	1973.82	2-0 P 7
50523.0	1979.29	5-1 P25	50663.6	1973.80	2-0 P 7
50523.6	1979.27	5-1 P25	50667.7	1973.64	2-0 R 9
50527.4	1979.13	5-1 R27	50667.7	1973.64	2-0 R 9
50527.7	1979.11	5-1 R27	50668.3	1973.62	2-0 R 9
50528.5	1979.08	5-1 R27	50683.3	1973.04	2-0 P 5
50530.7	1978.99	2-0 P15	50683.4	1973.03	2-0 P 5
50530.7	1978.99	2-0 P15	50683.7	1973.02	2-0 P 5
50531.3	1978.97	2-0 P15	50686.8	1972.90	2-0 R 7
50539.2	1978.66	2-0 R17	50686.8	1972.90	2-0 R 7
50539.3	1978.66	2-0 R17	50687.3	1972.88	2-0 R 7
50540.1	1978.63	2-0 R17	50698.1	1972.46	2-0 P 3
50550			50698.3	1972.45	2-0 P 3
50571.7	1977.39	2-0 P13	50698.6	1972.44	2-0 P 3
50571.7	1977.39	2-0 P13	50700		
50572.2	1977.37	2-0 P13	50700.6	1972.37	2-0 R 5
50579.2	1977.10	2-0 R15	50700.6	1972.36	2-0 R 5
50579.3	1977.09	2-0 R15	50701.1	1972.35	2-0 R 5
50580.0	1977.07	2-0 R15	50707.9	1972.08	2-0 P 1
50593.0	1976.56	5-1 P23	50709.1	1972.03	2-0 R 3
50593.1	1976.55	5-1 P23	50709.3	1972.03	2-0 R 3
50593.6	1976.53	5-1 P23	50709.7	1972.01	2-0 R 3
50597.2	1976.39	5-1 R25	50710.9	1971.96	2-0 Q 1
50597.5	1976.38	5-1 R25	50712.5	1971.90	2-0 R 1
50598.2	1976.35	5-1 R25	50712.6	1971.90	2-0 R 1
50600			50716.7	1971.74	5-1 P19
50607.4	1976.00	2-0 P11	50716.7	1971.74	5-1 P19
50607.4	1975.99	2-0 P11	50717.2	1971.72	5-1 P19
50607.9	1975.98	2-0 P11	50720.4	1971.59	5-1 R21
50613.9	1975.74	2-0 R13	50720.6	1971.59	5-1 R21
50614.0	1975.74	2-0 R13	50721.2	1971.56	5-1 R21
50614.6	1975.71	2-0 R13	50726.9	1971.34	3-0 P29
50637.9	1974.81	2-0 P 9	50727.1	1971.33	3-0 P29
50638.0	1974.80	2-0 P 9	50727.9	1971.30	3-0 P29
50638.4	1974.79	2-0 P 9			
50643.4	1974.59	2-0 R11			
50643.5	1974.59	2-0 R11			
50644.1	1974.57	2-0 R11			
50650					
50657.6	1974.04	5-1 P21			
50657.6	1974.04	5-1 P21			
50658.1	1974.02	5-1 P21			
50661.6	1973.88	5-1 R23			
50661.8	1973.87	5-1 R23			
50662.5	1973.85	5-1 R23			
50663.2	1973.82	2-0 P 7			

TABLE 7.- Identification of O_2 Schumann-Runge rotational lines 51750 - 52000 cm^{-1}.

ν	λ	band	ν	λ	band
51750					
51782.7	1931.15	4-0 P15	51909.1	1926.45	5-0 P29
51782.9	1931.14	4-0 P15	51909.7	1926.42	5-0 P29
51783.4	1931.12	4-0 P15	51911.4	1926.36	8-1 P29
51787.1	1930.98	4-0 R17	51911.9	1926.34	8-1 P29
51787.4	1930.97	4-0 R17	51912.5	1926.32	8-1 P29
51788.0	1930.95	4-0 R17	51920.5	1926.02	4-0 P 7
51796.0	1930.65	7-1 R21	51920.6	1926.02	4-0 P 7
51796.3	1930.64	7-1 R21	51920.9	1926.01	4-0 P 7
51797.0	1930.61	7-1 R21	51922.9	1925.93	4-0 R 9
51798.7	1930.55	7-1 P19	51923.0	1925.93	4-0 R 9
51798.8	1930.55	7-1 P19	51923.5	1925.91	4-0 R 9
51799.3	1930.53	7-1 P19	51941.3	1925.25	4-0 P 5
51800			51941.3	1925.25	4-0 P 5
51825.4	1929.56	4-0 P13	51941.7	1925.24	4-0 P 5
51825.5	1929.55	4-0 P13	51943.1	1925.18	4-0 R 7
51826.0	1929.54	4-0 P13	51943.2	1925.18	4-0 R 7
51829.3	1929.41	4-0 R15	51943.6	1925.16	4-0 R 7
51829.5	1929.40	4-0 R15	51948.6	1924.98	7-1 R15
51830.1	1929.38	4-0 R15	51948.8	1924.97	7-1 R15
51850			51949.3	1924.96	7-1 R15
51852.7	1928.54	7-1 R19	51950		
51853.0	1928.53	7-1 R19	51950.2	1924.92	7-1 P13
51853.6	1928.51	7-1 R19	51950.3	1924.92	7-1 P13
51855.0	1928.46	7-1 P17	51950.6	1924.90	7-1 P13
51855.1	1928.45	7-1 P17	51956.6	1924.68	4-0 P 3
51855.5	1928.43	7-1 P17	51956.6	1924.68	4-0 P 3
51862.6	1928.17	4-0 P11	51957.1	1924.67	4-0 P 3
51862.6	1928.17	4-0 P11	51957.9	1924.64	4-0 R 5
51863.1	1928.15	4-0 P11	51957.9	1924.63	4-0 R 5
51865.9	1928.05	4-0 R13	51958.4	1924.62	4-0 R 5
51866.1	1928.04	4-0 R13	51966.4	1924.32	4-0 P 1
51866.7	1928.02	4-0 R13	51967.2	1924.29	4-0 R 3
51894.3	1926.99	4-0 P 9	51967.2	1924.29	4-0 R 3
51894.3	1926.99	4-0 P 9	51967.6	1924.27	4-0 R 3
51894.7	1926.98	4-0 P 9	51969.4	1924.21	4-0 Q 1
51897.1	1926.89	4-0 R11	51971.0	1924.15	4-0 R 1
51897.3	1926.88	4-0 R11	51971.0	1924.15	4-0 R 1
51897.8	1926.86	4-0 R11	51987.8	1923.53	7-1 R13
51900			51987.9	1923.52	7-1 R13
51903.6	1926.65	7-1 R17	51988.4	1923.51	7-1 R13
51903.8	1926.64	7-1 R17	51989.1	1923.48	7-1 P11
51904.3	1926.62	7-1 R17	51989.1	1923.48	7-1 P11
51905.5	1926.58	7-1 P15	51989.5	1923.47	7-1 P11
51905.6	1926.57	7-1 P15	51989.7	1923.46	8-1 R29
51906.0	1926.56	7-1 P15	51990.4	1923.43	8-1 R29
51908.9	1926.45	5-0 P29	51991.2	1923.40	8-1 R29

TABLE 8.- Identification of O_2 Schumann-Runge rotational lines 54000 - 54250 cm^{-1}.

TABLE 8

IDENTIFICATION OF O_2 SCHUMANN-RUNGE ROTATIONNAL LINES
54000 - 54250 cm^{-1}

ν	λ	band	ν	λ	band	ν	λ	band
54000								
54000.0	1851.85	8-0 P13	54092.9	1848.67	15-1 P29	54153.1	1846.62	8-0 P 1
54000.2	1851.85	8-0 P13	54094.3	1848.62	14-1 R27	54153.1	1846.62	15-1 R29
54000.5	1851.84	8-0 P13	54100			54155.8	1846.52	8-0 Q 1
54003.7	1851.73	12-1 P15	54100.8	1848.40	15-1 P29	54157.2	1846.48	8-0 R 1
54004.9	1851.68	12-1 P15	54101.1	1848.39	8-0 R 9	54157.4	1846.47	8-0 R 1
54005.4	1851.67	12-1 P15	54101.3	1848.39	8-0 R 9	54158.0	1846.45	9-0 P23
54006.9	1851.62	13-1 P23	54101.4	1848.38	12-1 P11	54158.4	1846.44	9-0 P23
54008.5	1851.56	13-1 P23	54101.6	1848.38	8-0 R 9	54158.7	1846.43	9-0 P23
54035.9	1850.62	14-1 P27	54102.5	1848.34	12-1 P11	54161.1	1846.35	12-1 R 9
54036.4	1850.61	8-0 R13	54102.7	1848.34	12-1 P11	54162.1	1846.31	12-1 R 9
54036.6	1850.60	8-0 R13	54104.0	1848.29	8-0 P 7	54162.4	1846.30	12-1 R 9
54037.0	1850.59	8-0 R13	54104.1	1848.29	8-0 P 7	54164.6	1846.22	13-1 P19
54038.0	1850.55	12-1 R15	54104.4	1848.28	8-0 P 7	54167.0	1846.14	13-1 P19
54039.4	1850.50	12-1 R15	54124.3	1847.60	8-0 R 7	54168.1	1846.10	13-1 P19
54040.0	1850.48	12-1 R15	54124.4	1847.59	8-0 R 7	54171.5	1845.99	12-1 P 7
54040.8	1850.45	8-0 P11	54124.7	1847.58	8-0 R 7	54172.4	1845.96	12-1 P 7
54040.9	1850.45	14-1 P27	54126.5	1847.52	8-0 P 5	54172.5	1845.96	12-1 P 7
54041.2	1850.44	8-0 P11	54126.6	1847.52	8-0 P 5	54185.8	1845.50	14-1 R25
54044.0	1850.34	14-1 P27	54126.9	1847.51	8-0 P 5	54188.2	1845.42	12-1 R 7
54050			54127.0	1847.51	12-1 R11	54189.2	1845.39	12-1 R 7
54051.2	1850.10	13-1 R23	54128.2	1847.47	12-1 R11	54189.4	1845.38	12-1 R 7
54054.4	1849.99	13-1 R23	54128.6	1847.45	12-1 R11	54190.9	1845.33	14-1 R25
54056.0	1849.93	12-1 P13	54131.5	1847.35	13-1 R21	54194.1	1845.22	14-1 R25
54056.5	1849.92	13-1 R23	54134.4	1847.26	13-1 R21	54196.1	1845.15	12-1 P 5
54057.2	1849.89	12-1 P13	54136.1	1847.20	13-1 R21	54197.0	1845.12	12-1 P 5
54057.5	1849.88	12-1 P13	54138.6	1847.11	15-1 R29	54197.1	1845.12	12-1 P 5
54062.6	1849.71	9-0 R27	54139.8	1847.07	14-1 P25	54200		
54063.2	1849.69	9-0 R27	54139.9	1847.07	12-1 P 9	54204.2	1844.88	13-1 R19
54063.7	1849.67	9-0 R27	54140.9	1847.03	12-1 P 9	54206.9	1844.79	13-1 R19
54071.8	1849.39	8-0 R11	54141.0	1847.03	12-1 P 9	54208.4	1844.73	13-1 R19
54072.0	1849.39	8-0 R11	54141.4	1847.02	8-0 R 5	54208.4	1844.73	12-1 R 5
54072.3	1849.38	8-0 R11	54141.5	1847.01	8-0 R 5	54209.3	1844.70	12-1 R 5
54075.5	1849.27	8-0 P 9	54141.8	1847.00	8-0 R 5	54209.5	1844.70	12-1 R 5
54075.6	1849.26	8-0 P 9	54142.9	1846.96	8-0 P 3	54210.7	1844.65	15-1 P27
54075.9	1849.25	8-0 P 9	54143.0	1846.96	8-0 P 3	54213.8	1844.55	12-1 P 3
54078.2	1849.17	9-0 P25	54143.5	1846.94	8-0 P 3	54214.7	1844.52	12-1 P 3
54078.7	1849.16	9-0 P25	54143.7	1846.94	9-0 R25	54215.2	1844.50	12-1 P 3
54079.0	1849.15	9-0 P25	54144.3	1846.92	9-0 R25	54217.5	1844.42	16-1 P29
54084.9	1848.95	14-1 R27	54144.4	1846.91	14-1 P25	54217.9	1844.41	15-1 P27
54086.0	1848.91	12-1 R13	54144.7	1846.90	9-0 R25	54218.4	1844.39	9-0 R23
54087.3	1848.86	12-1 R13	54147.1	1846.82	14-1 P25	54219.0	1844.37	9-0 R23
54087.8	1848.85	12-1 R13	54147.4	1846.81	15-1 R29	54219.4	1844.36	9-0 R23
54088.0	1848.84	13-1 P21	54150			54221.6	1844.28	12-1 R 3
54090.6	1848.75	14-1 R27	54152.4	1846.64	8-0 R 3	54222.2	1844.26	15-1 P27
54090.6	1848.75	13-1 P21	54152.5	1846.64	8-0 R 3	54222.5	1844.25	12-1 R 3
54092.0	1848.70	13-1 P21	54152.9	1846.62	8-0 R 3	54222.8	1844.24	12-1 R 3

comparison at 300 K between the calculated and measured cross sections. The calculations also make it possible to determine the respective role of the lines and of the continuum in the O_2 absorption cross section (Fig. 1b) where variations of $\pm$ 10 and $\pm$ 20% in the underlying continuum are depicted. Other figures have been published for temperatures between 270 K and 190 K (Examples, fig. 1c and 1d) in order to define for each spectral interval the exact role of the underlying continuum at varying temperatures adopted to atmospheric conditions. Finally, figures 2b and 3b illustrate the variations in the structure of the absorption spectrum from the laboratory temperature 300 K to atmospheric temperatures 270, 230 and 190 K. It is possible to follow easily with decreasing temperature, the marked variations in the absorption of the rotation lines starting from the vibrational level v" = 1.

The spectral interval 50500 - 50750 cm^{-1} (Table 6 and Fig. 1a, b, c and d) corresponds mainly to the 2-0 band with an effect of the 5-1 band at 300 K. The experimental structure for absorption less than 2×10^{-23} cm^2 is due to laboratory noise. The effect of the underlying Herzberg continuum is important since it can be detected easily by the differences of $\pm$ 10 and $\pm$ 20% illustrated in figure 1b particularly by the absolute values of the absorption cross section with and without continuum at 270 K and 190 K as depicted in Fig. 1c and 1d.

The spectral interval 51750 - 52000 cm^{-1} is characterized by linewidths ($\Delta\nu$ = 3.6 cm^{-1}) of the rotational lines of the 4-0 band (Table 7). These lines play a very important role in the overall pattern of absorption (Fig. 2a), since the effect of the Herzberg continuum is negligible and produces practically no variation when the absorption cross section are varied by $\pm$ 10 or $\pm$ 20%. The variation of the absorption cross section with temperature (T = 300, 270, 230 to 190 K) illustrates the decreasing role of the 7-1 band (Fig. 2b) and the change in the structure of the 4-0 band at high rotational levels, P15-R17.

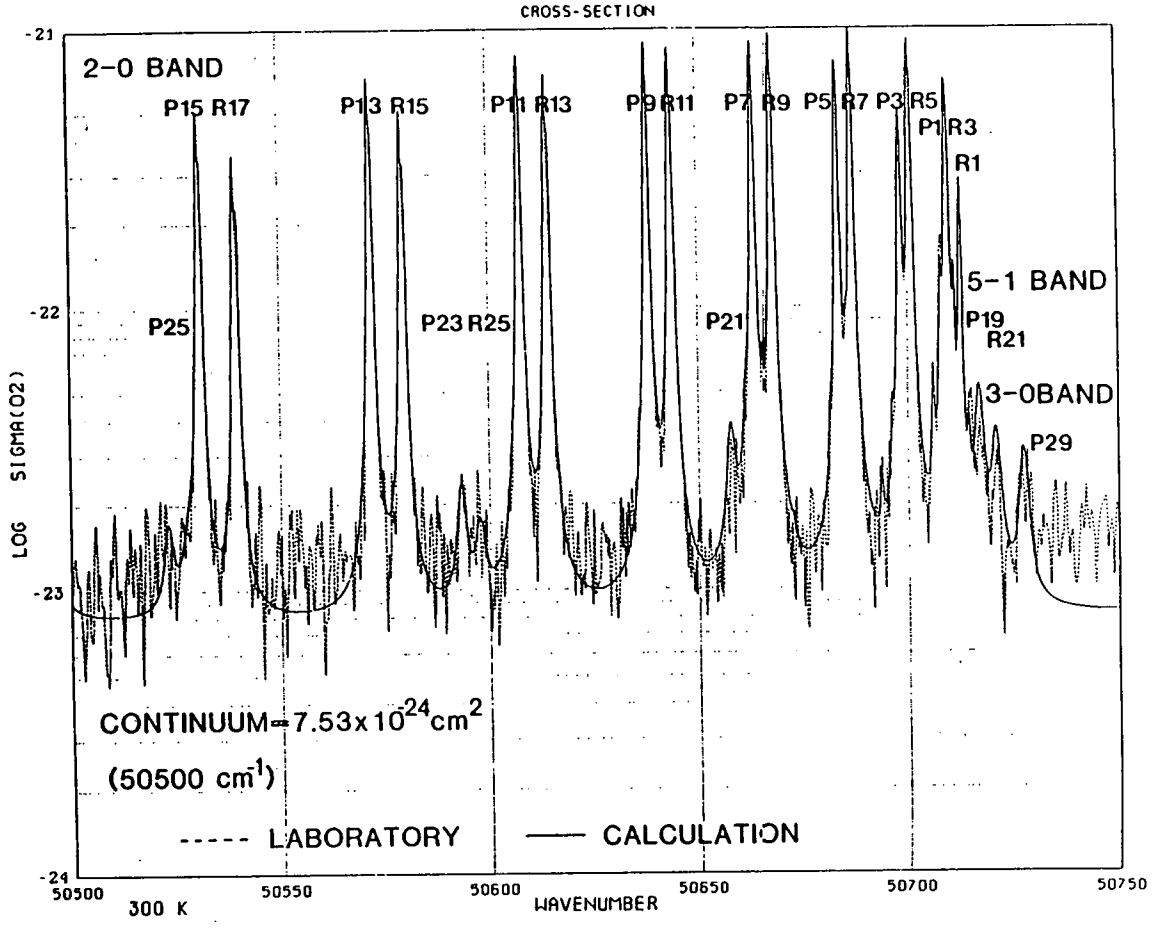

Fig. 1a.- Theoretical and experimental absorption cross sections of the 2-0 Schumann-Runge band of O_2 between 50500 and 50750 cm^{-1} at 300 K. Oscillator strength and linewidth 1.9 x 10^{-5} and 0.6 cm^{-1}, respectively. Strong effect of the Herzberg continuum.

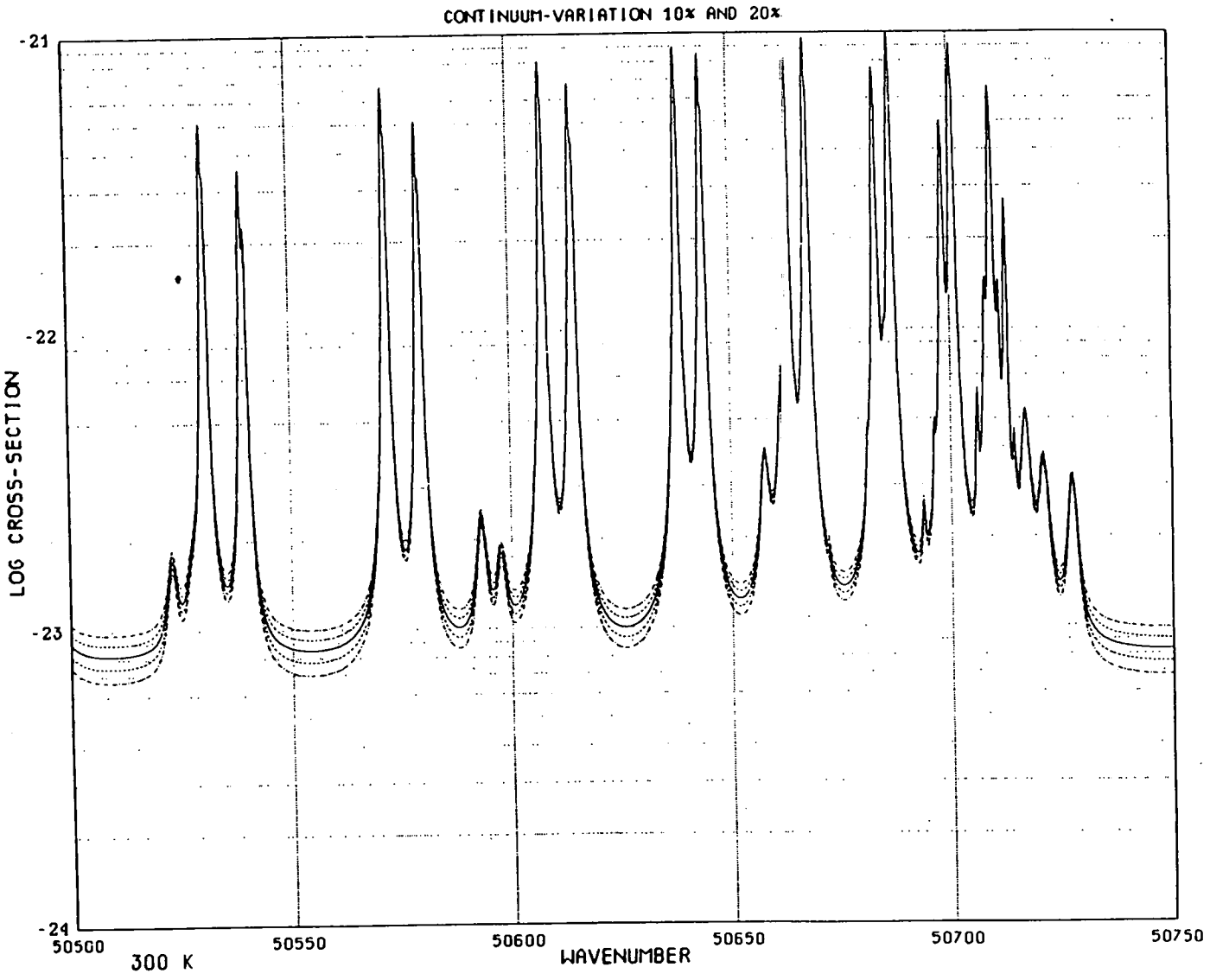

Fig. 1b.- Absorption structure of the 2-0 band with variations of ± 10 and ± 20% in the cross section of the underlying continuum at 300 K. Obvious role of the continuum with its differences.

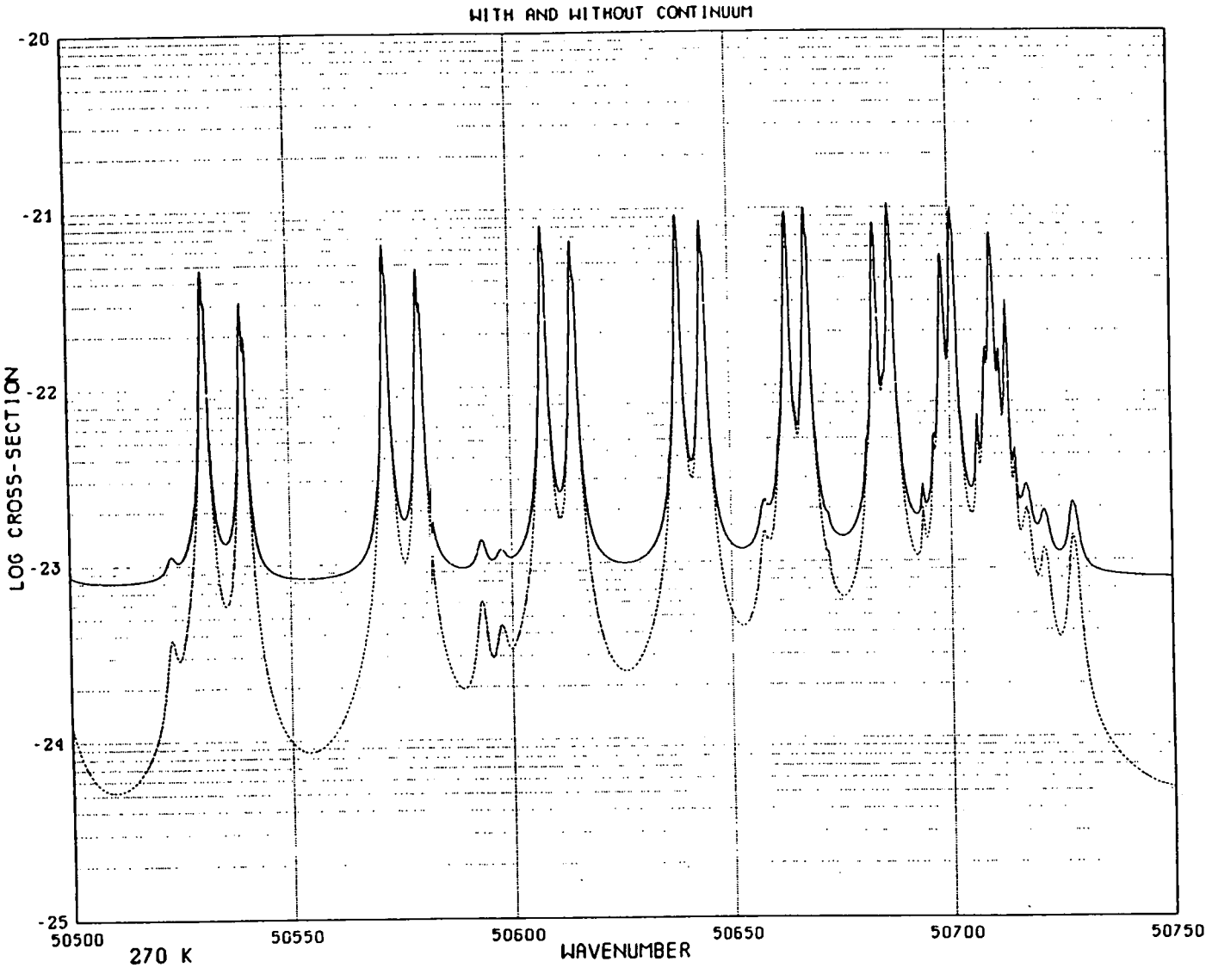

Fig. 1c.- Absorption structure with and without continuum between 50500 and 50750 cm^{-1} at 270 K.
Differences of a factor of 10 between lines at 50500 cm^{-1}.

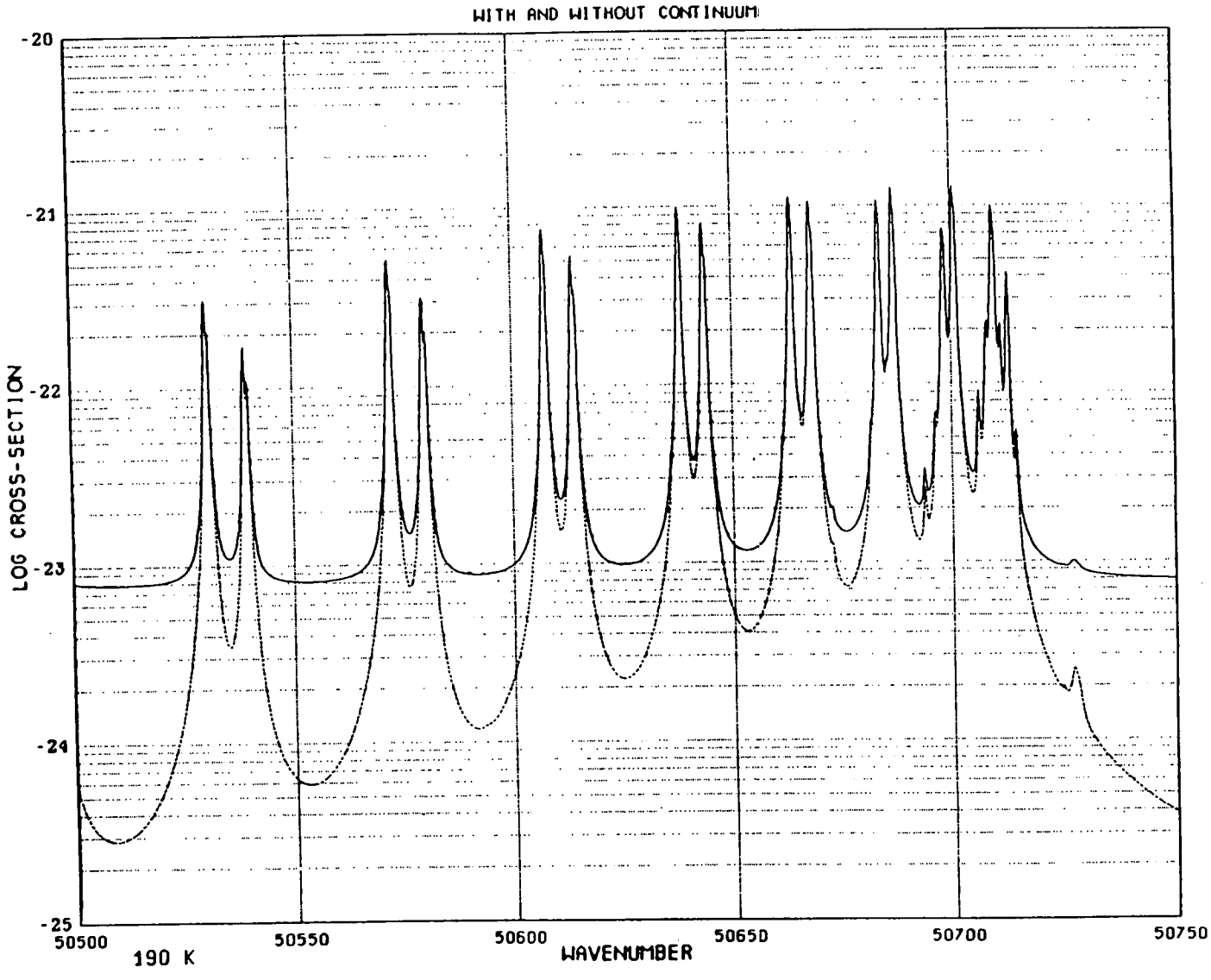

Fig. 1d.- Absorption structure with and without continuum between 50500 and 50750 cm^{-1} at 190 K.
Increase of differences at high rotation levels; cross sections reaching 3×10^{-25} cm^2 near 50500 cm^{-1}.

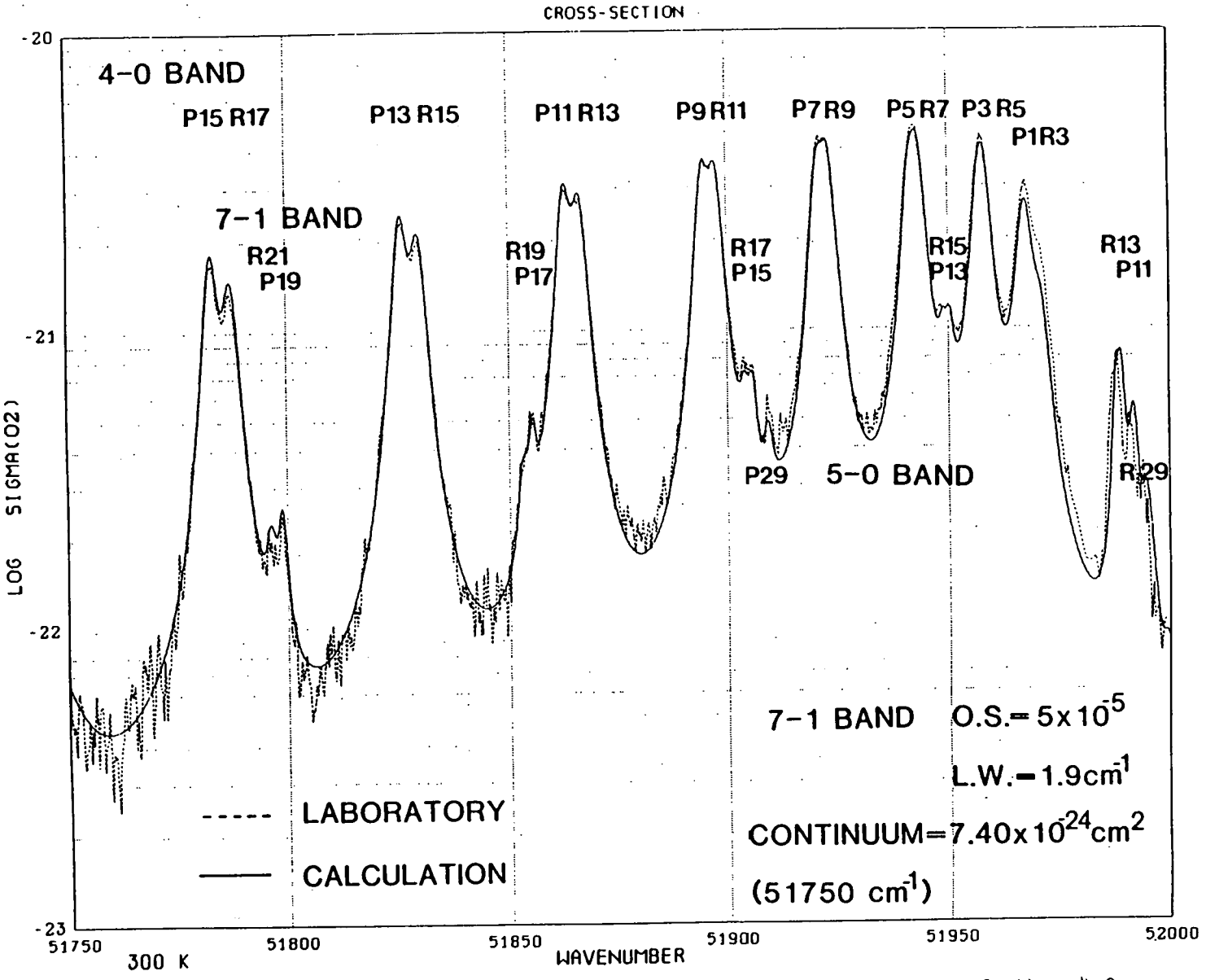

Fig. 2a.- Theoretical and experimental absorption cross sections of the 4-0 Schumann-Runge band of O_2 between 51750 and 52000 cm^{-1} at 300 K. Oscillator strength and linewidth 2.7 x 10^{-7} and 3.6 cm^{-1}, respectively. Linewidths of 2-0 to be compared.

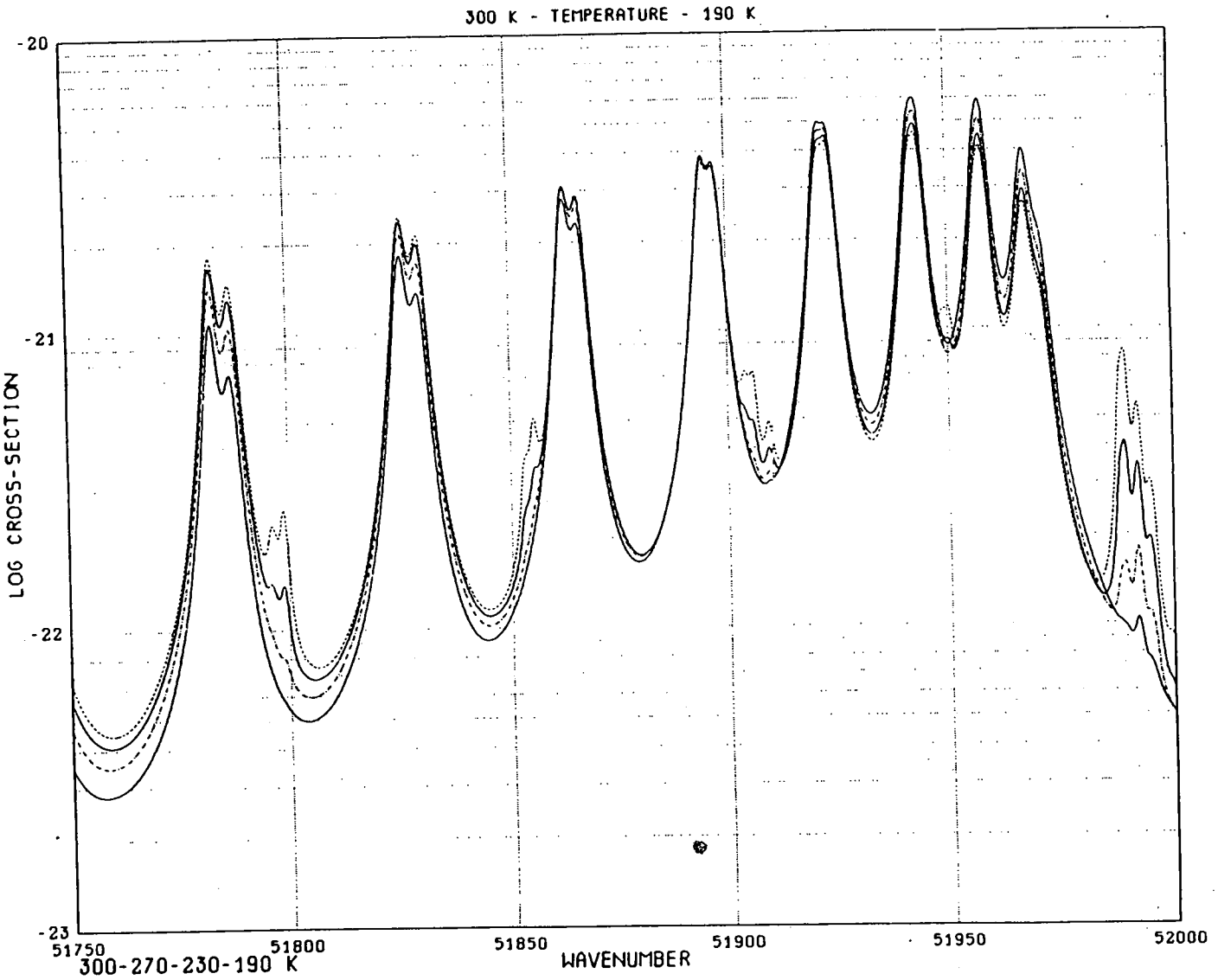

Fig. 2b.- Temperature effect on the rotational structure between 51750 and 52000 cm^{-1}.
Effects of a temperature decrease from 300 K to 270, 230 and 190 K on the 4-0 and 7-1 bands.

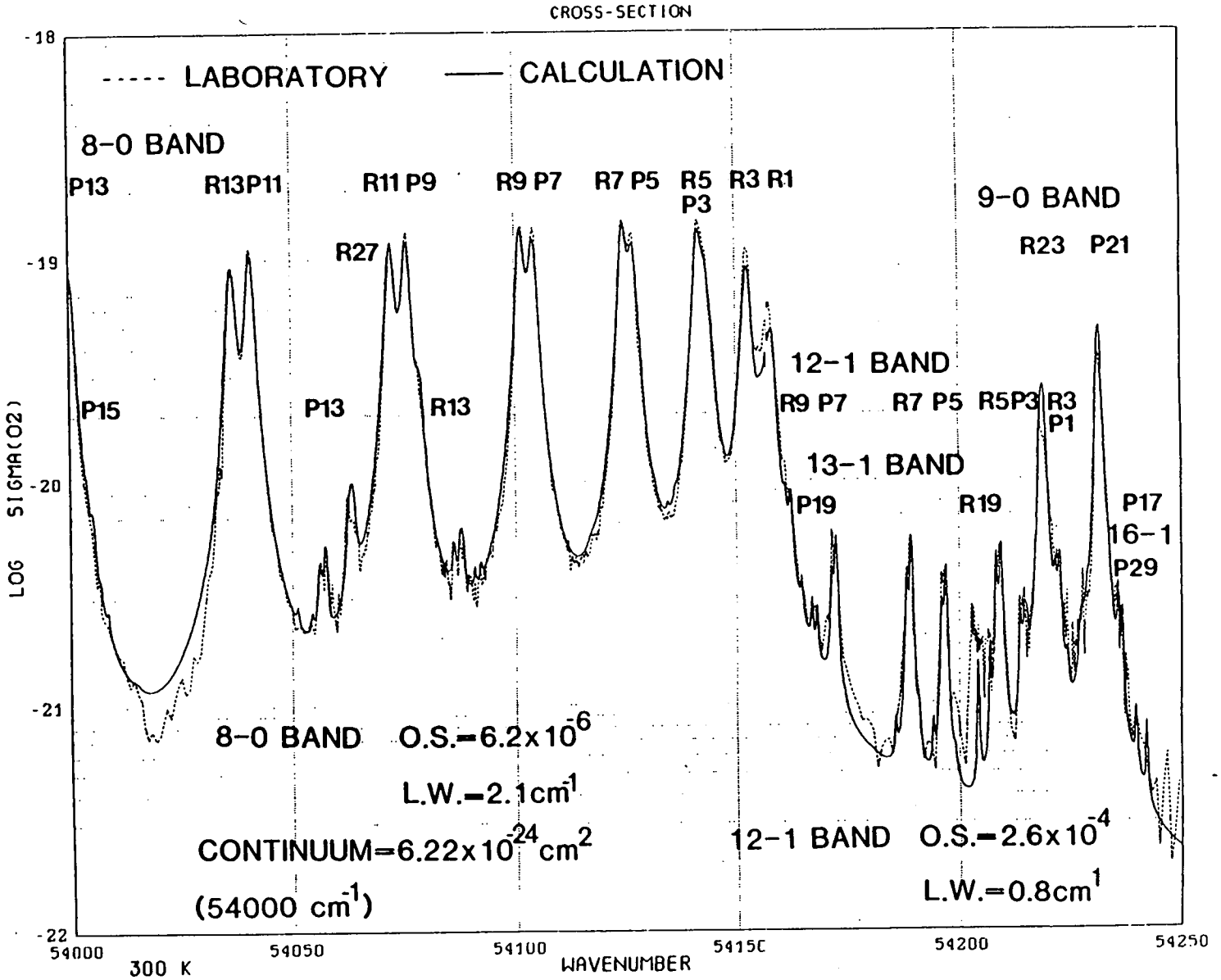

Fig. 3a.- Theoretical and experimental absorption cross sections of the 8-0 Schumann-Runge band of O_2 between 54000-54250 cm^{-1} at 300 K. No effect of the underlying continuum.

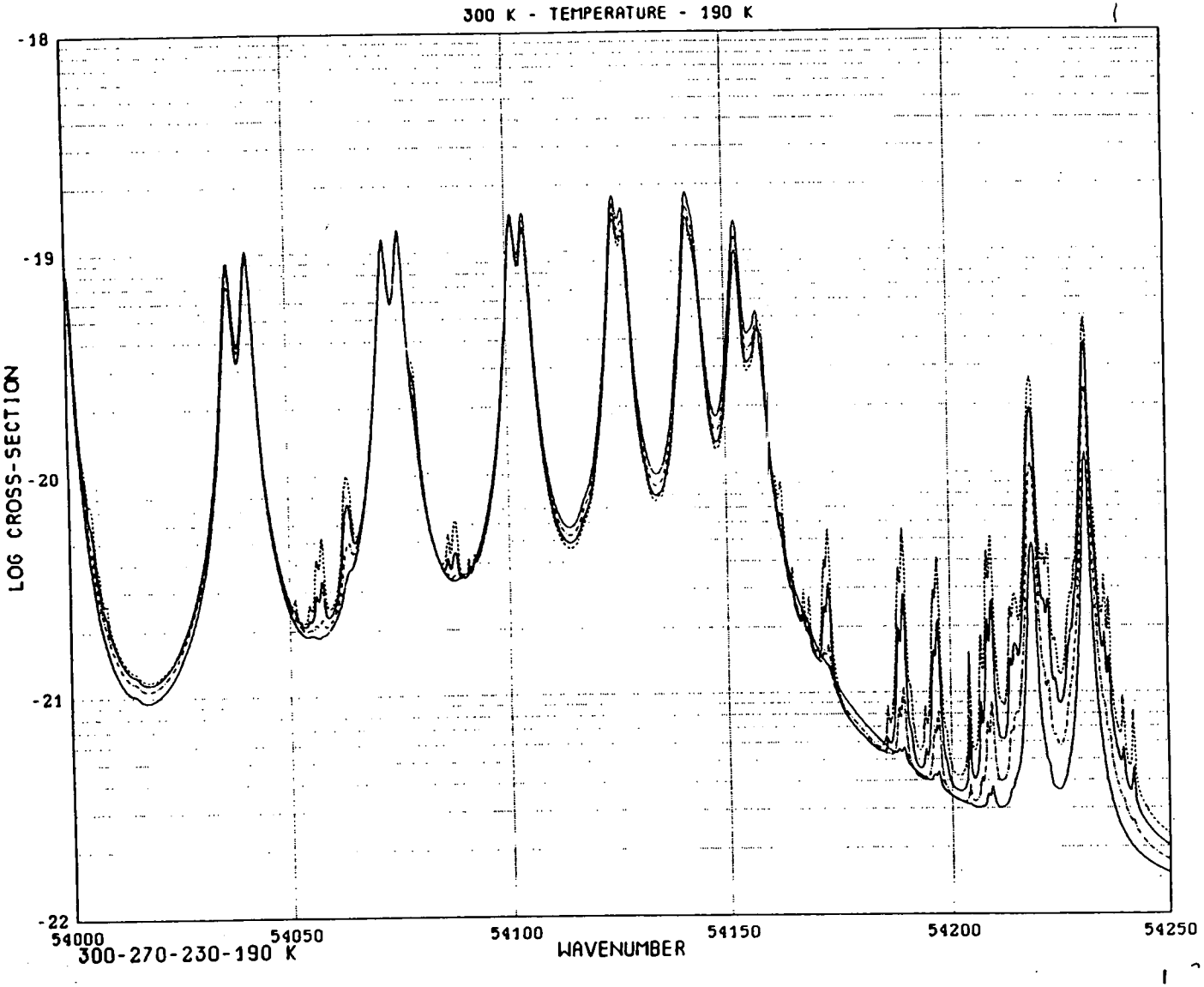

Fig. 3b.- Temperature effect on the rotational structure between 54000 and 54250 cm^{-1}.
Effects of a temperature decrease from 300 K to 270, 230 and 190 K particularly on the lines of the 12-1 and 13-1 bands.

In the 54000 - 54250 cm^{-1} interval, the principal contribution to the total absorption cross section corresponds to the P1 - P13 lines of the 8-0 band with an additional effect of the 12 - 1 and 13 - 1 bands (Fig. 3a). There is no contribution of the continuum (6×10^{-24} cm^2) since the minimum cross section is not less than 5×10^{-22} cm^2. The variation of the structure (Fig. 3b) is associated only with the rotational and vibrational populations related to temperatures (300 K to 190 K) particularly in the 54150 - 54250 cm^{-1} region corresponding to the lines of the (12 - 1), (13 - 1) and (14 - 1) bands.

It seems, therefore, that there is remarkable agreement between the experimental and theoretical cross sections. Yoshino et al., (1983) estimate that the errors in the spectral range 6 - 0 to 12 - 0 bands may vary from about 5% in regions of the principal absorption peaks to about 10% in window regions and that errors in the range of the absolute cross sections below 10^{-22} cm^2 could be somewhat greater. In any case, our detailed modeling procedure in which the cross section is computed as a function of wavenumber for lines with Voigt profiles and in which predissociation line widths are treated as parameters produces excellent agreement with the best experimental data independent of the instrumental width. It is also justified by a comparison of the theoretical and experimental cross sections at 79 K.

6. THE SCHUMANN-RUNGE BANDS AT 79 K

The recent experimental determination by Yoshino et al. (1987) of the cross sections at 79 K with an instrumental bandwith of 0.4 cm^{-1} has been compared with a theoretical calculation based on the spectroscopic parameters adopted at 300 K. We present our comparison in graphical format with a semi logarithmic plot for the 2 - 0 bands through 12 - 0 with a complete assigment of all rotation lines (Fig. 4 to 14). According to Yoshino et al. (1987) their experimental values of the absolute absorption cross sections would be of the order of 4% in regions of the principal absorption peaks while the errors in the range below 5×10^{-22} cm^{-1} should be greater (limited column density). This is the explanation

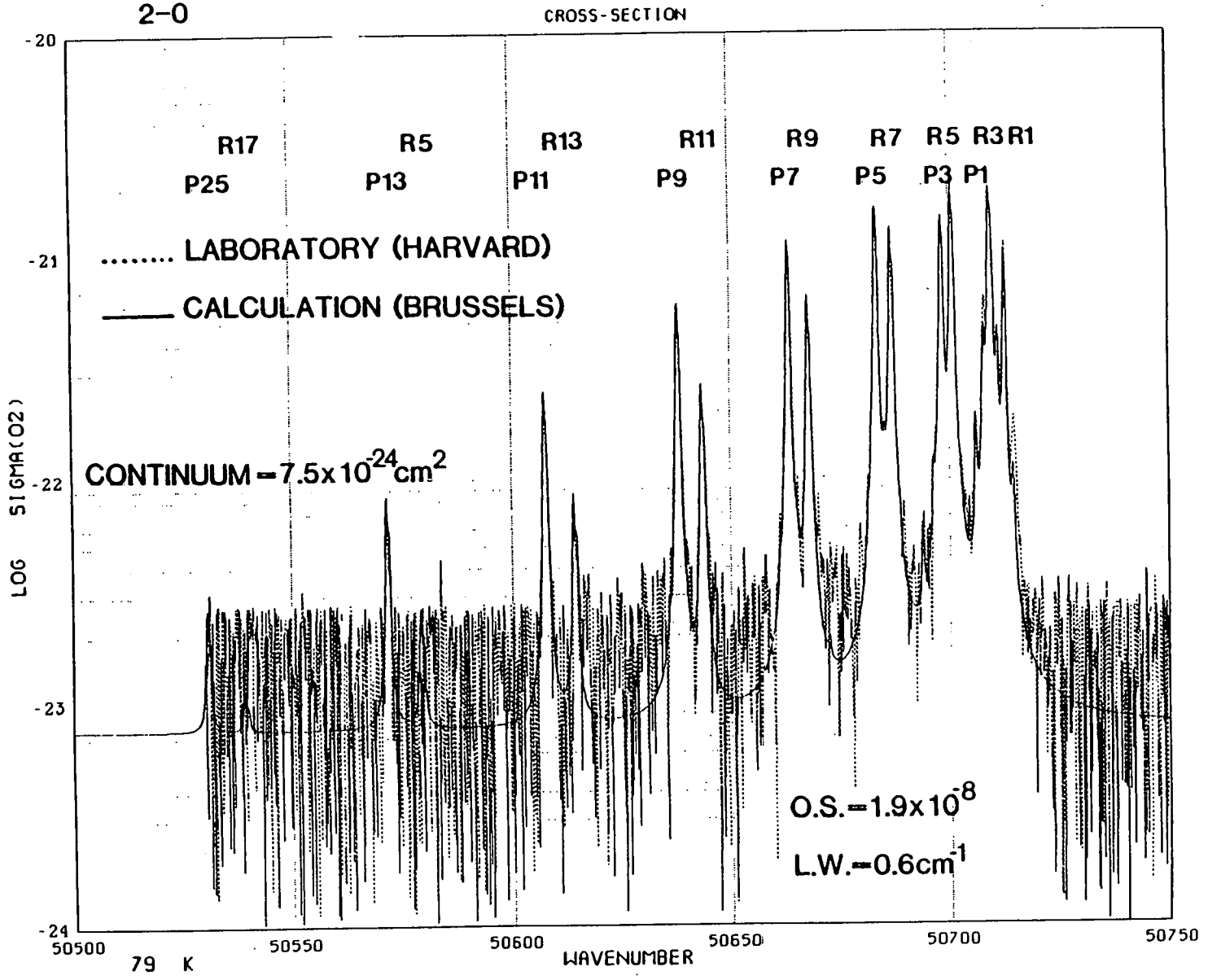

Fig. 4.- Absorption cross sections of the 2-0 band at 79 K. Experimental cross sections less than 5×10^{-23} cm^2 in the laboratory noise. Agreement between theoretical and experimental peaks.

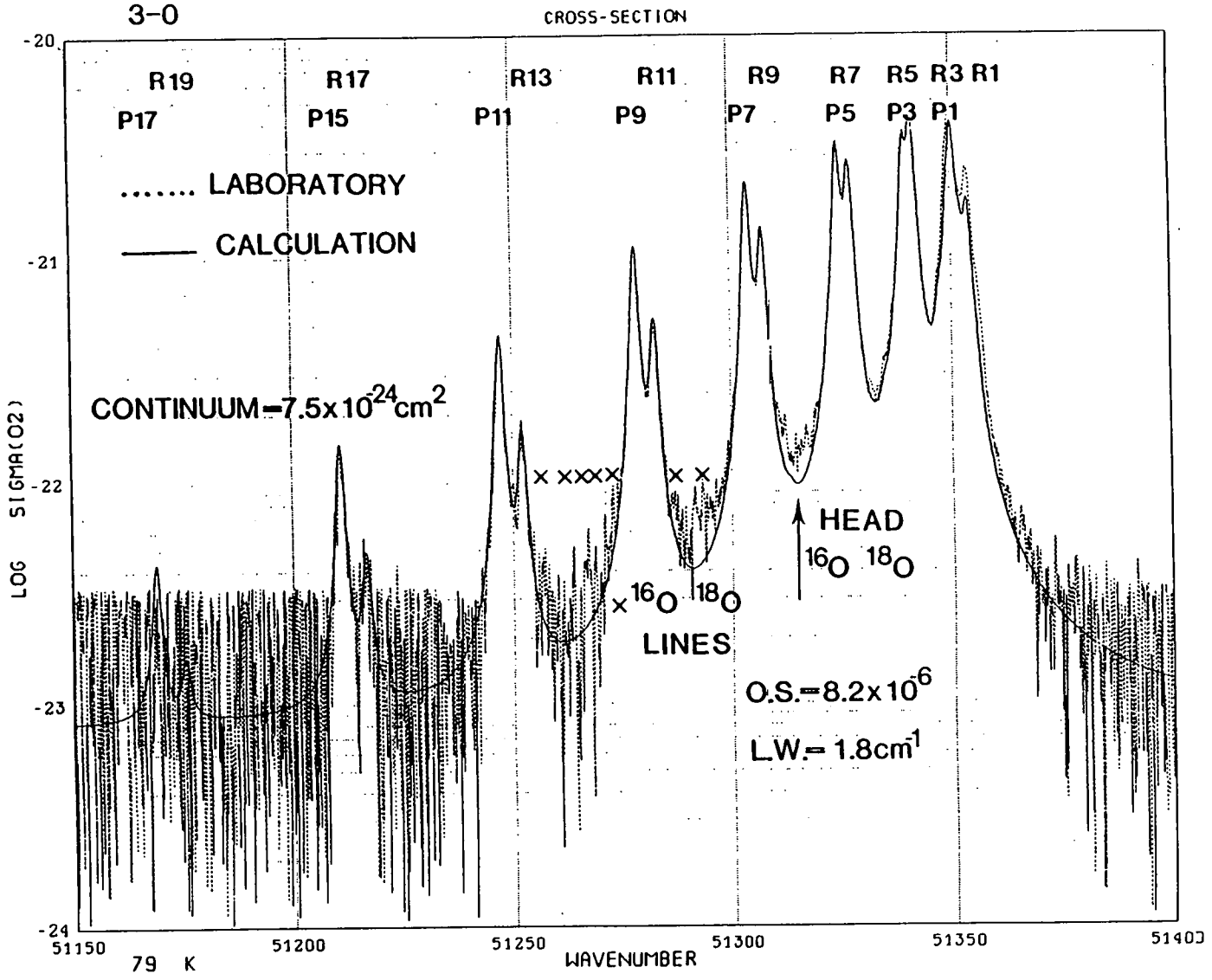

Fig. 5.- Absorption cross sections of the 3-0 band at 79 K. Rotation lines of $^{16}O\ ^{18}O$ isotope with spikes for cross sections not less than 5×10^{-23} cm^2.

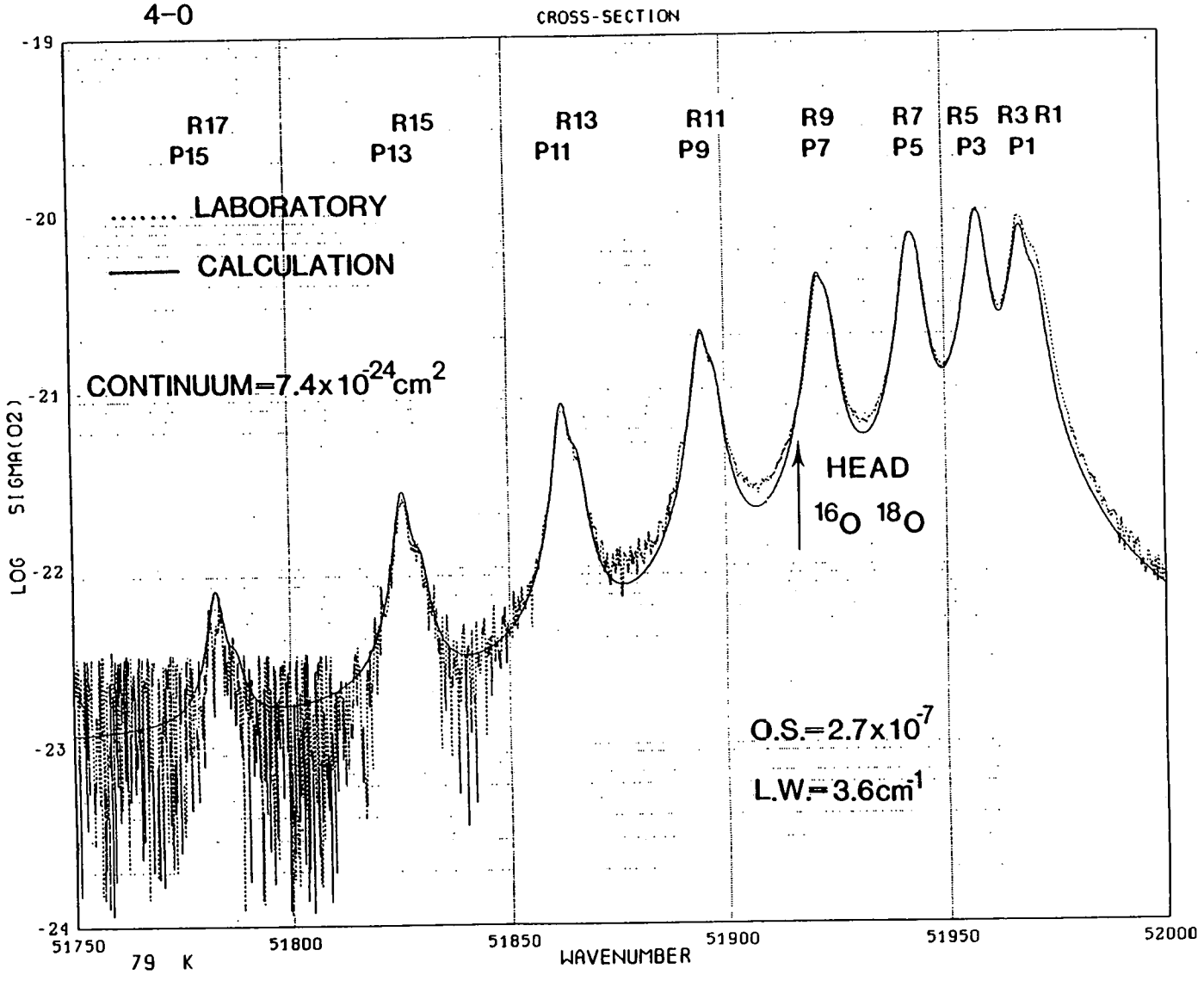

Fig. 6.- Absorption cross sections of the 4-0 banc at 79 K.
Linewidth determined at 300 K in agreement with structure at 79 K.

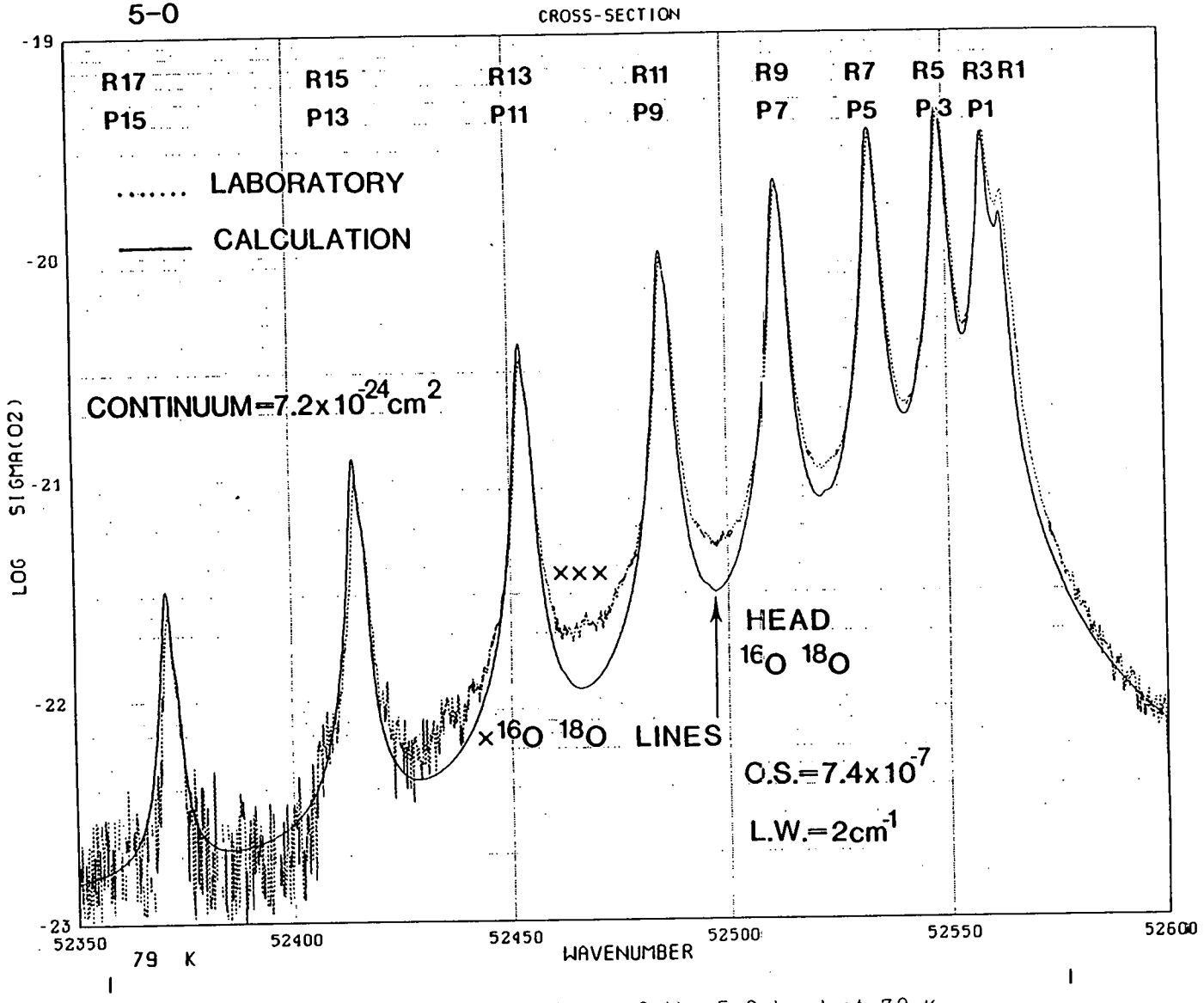

Fig. 7.- Absorption cross sections of the 5-0 band at 79 K. Underlying continuum (0.7×10^{-23} cm^2) without any effect.

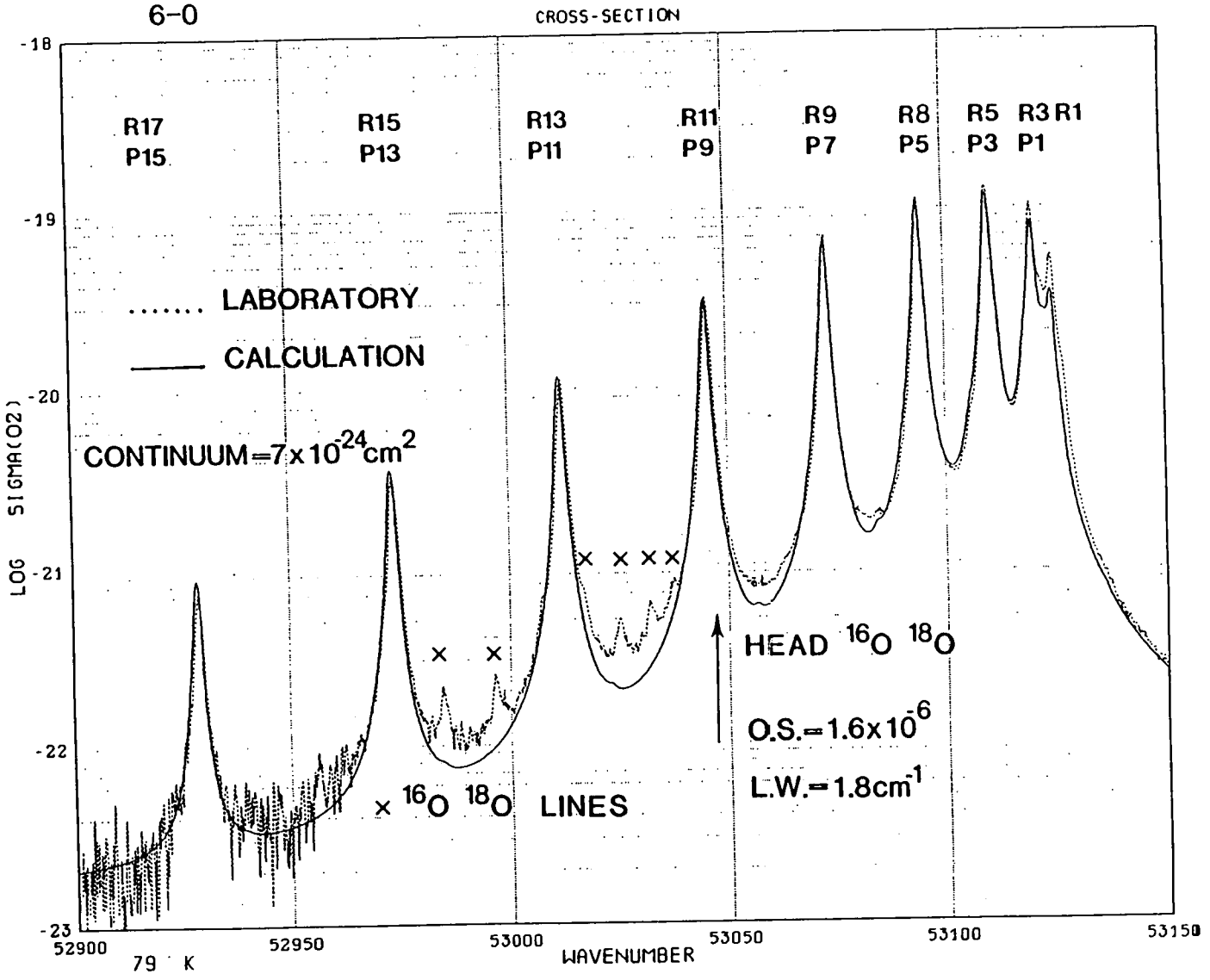

Fig. 8.- Absorption cross sections of the 6-0 band at 79 K. Spikes corresponding to $^{16}O\ ^{18}O$ lines clearly apparent between $^{16}O_2$ lines below the $^{16}O\ ^{18}O$ head.

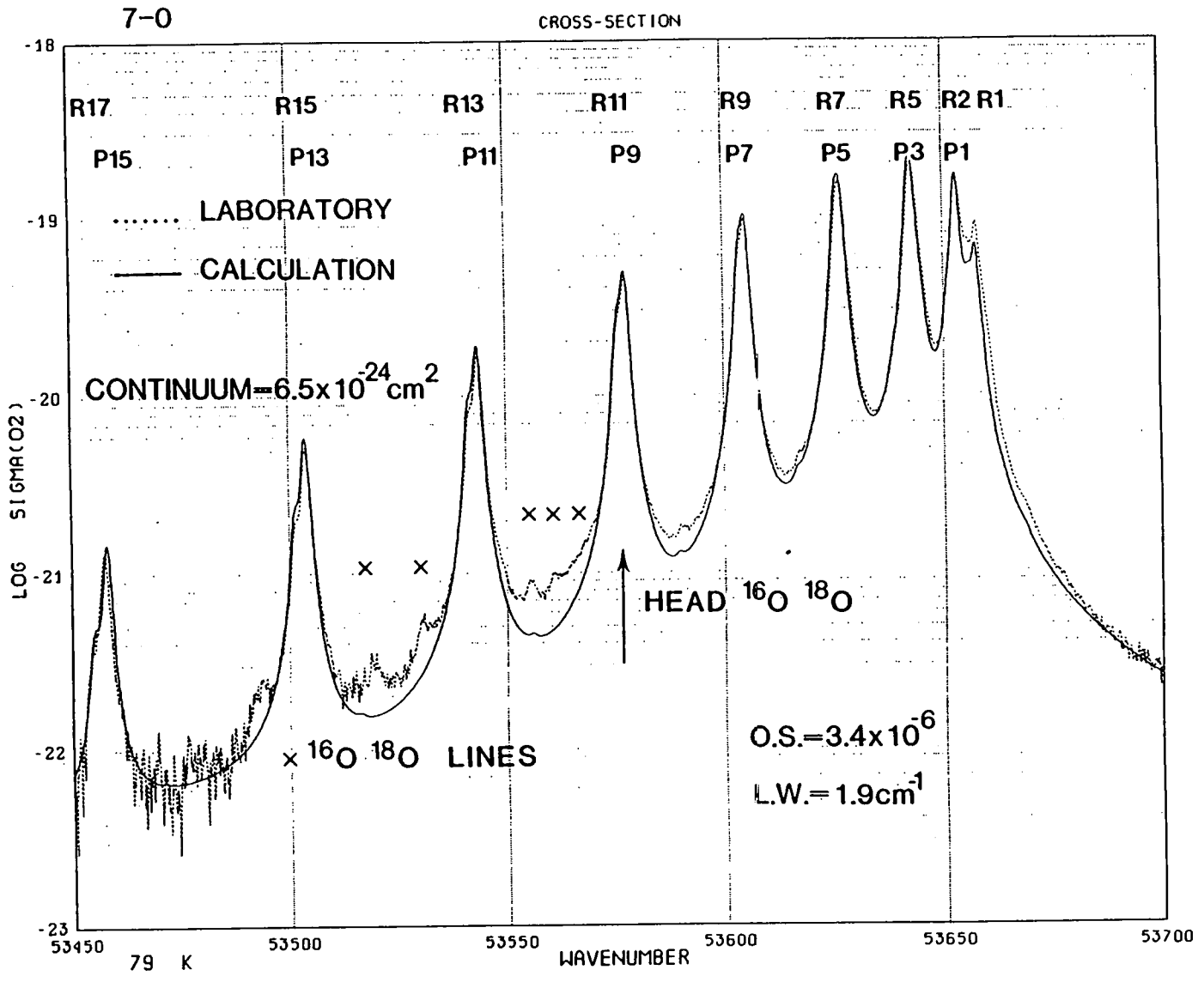

Fig. 9.- Absorption cross sections of the 7-0 band at 79 K. Laboratory noise still noticeable near 10^{-22} cm^2.

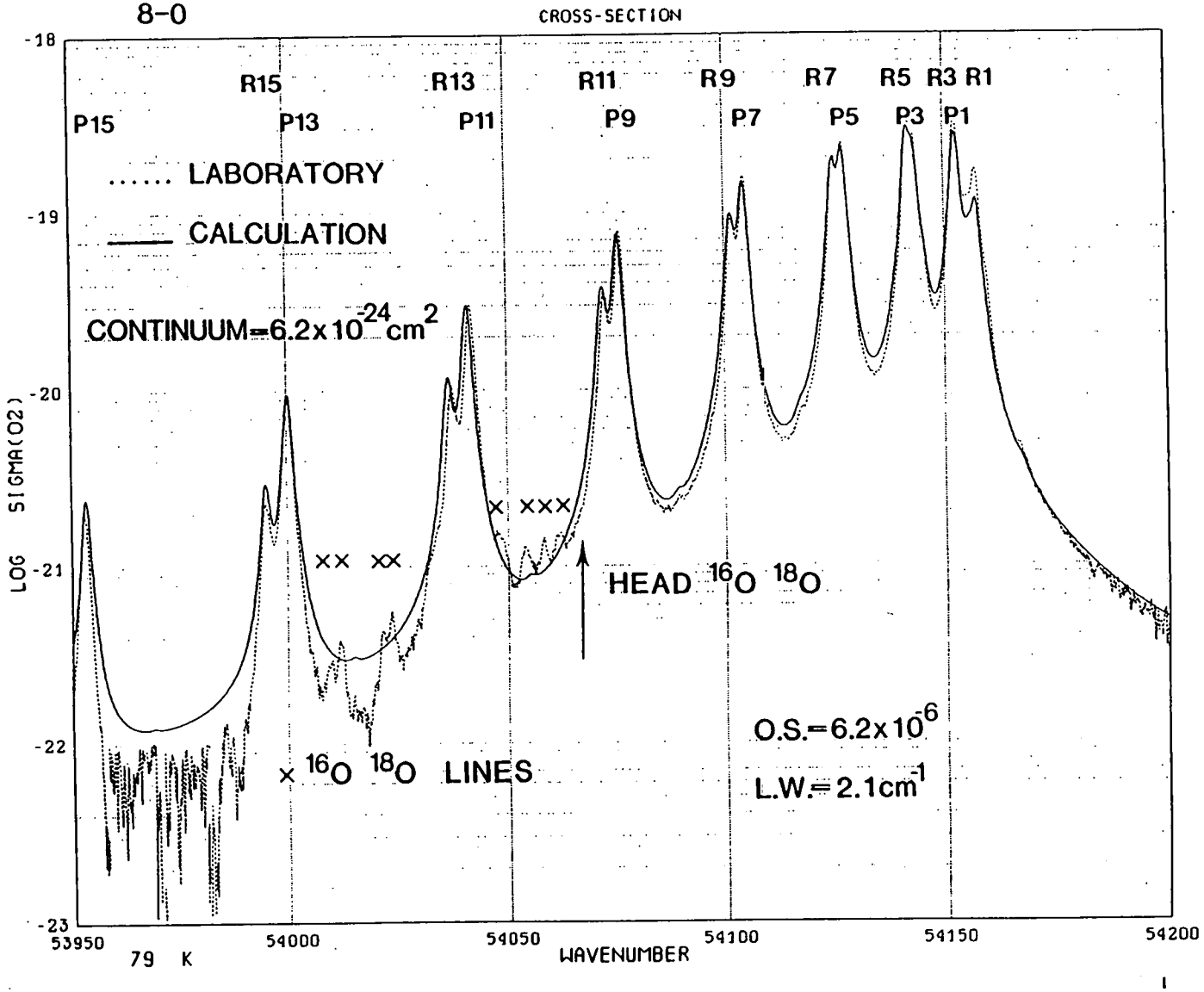

Fig. 10.- Absorption cross sections of the 8-0 band at 79 K.
Apparent anomaly between P13 and P15 lines as a result of the laboratory limited column density.

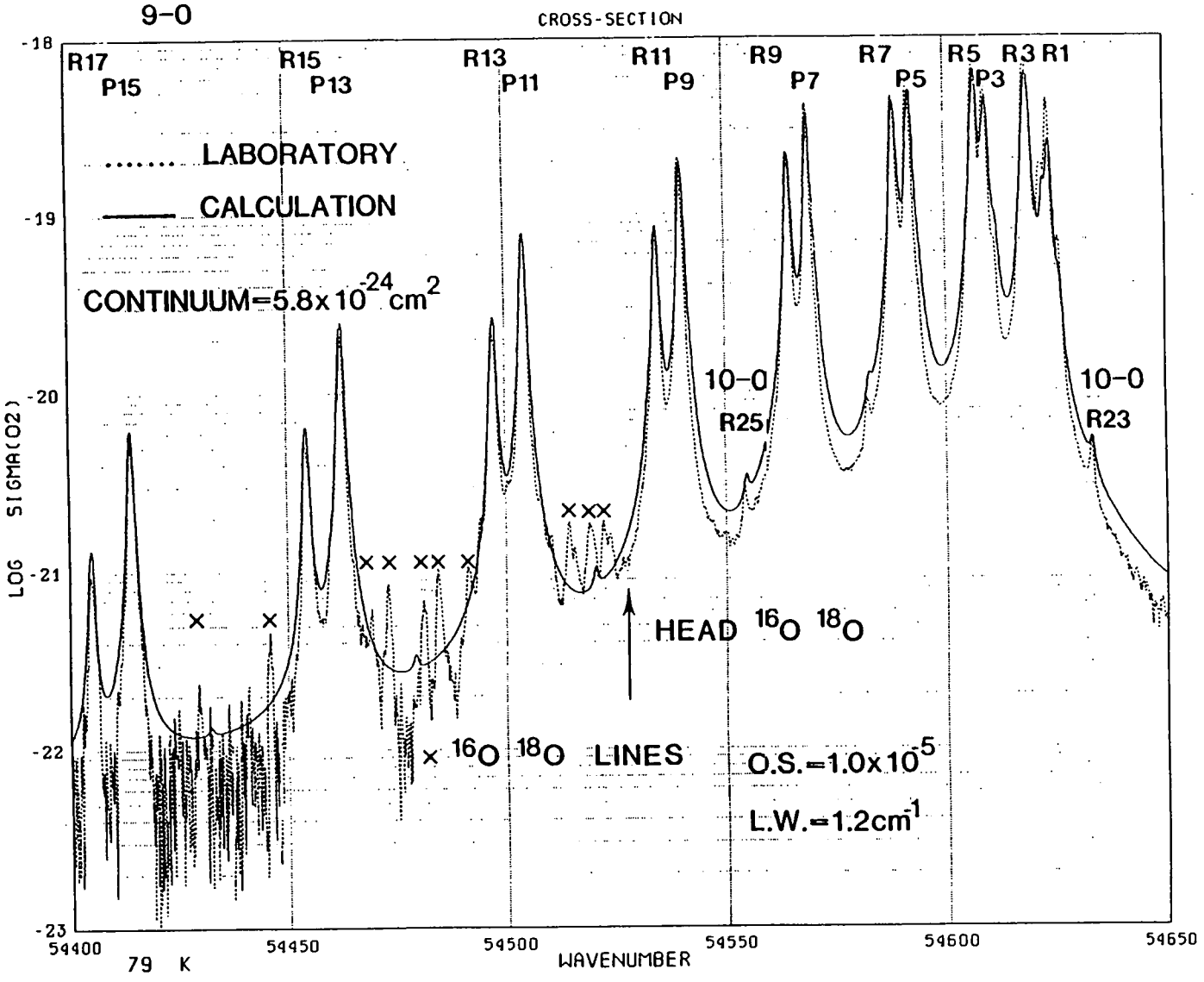

Fig. 11.- Absorption cross sections of the 9-0 band at 79 K. Superposition between P13 and R13 lines of $^{16}O\ ^{18}O$ spikes and laboratory noise, > 5 x 10^{-22} cm^2 and < 10^{-22} cm^2, respectively.

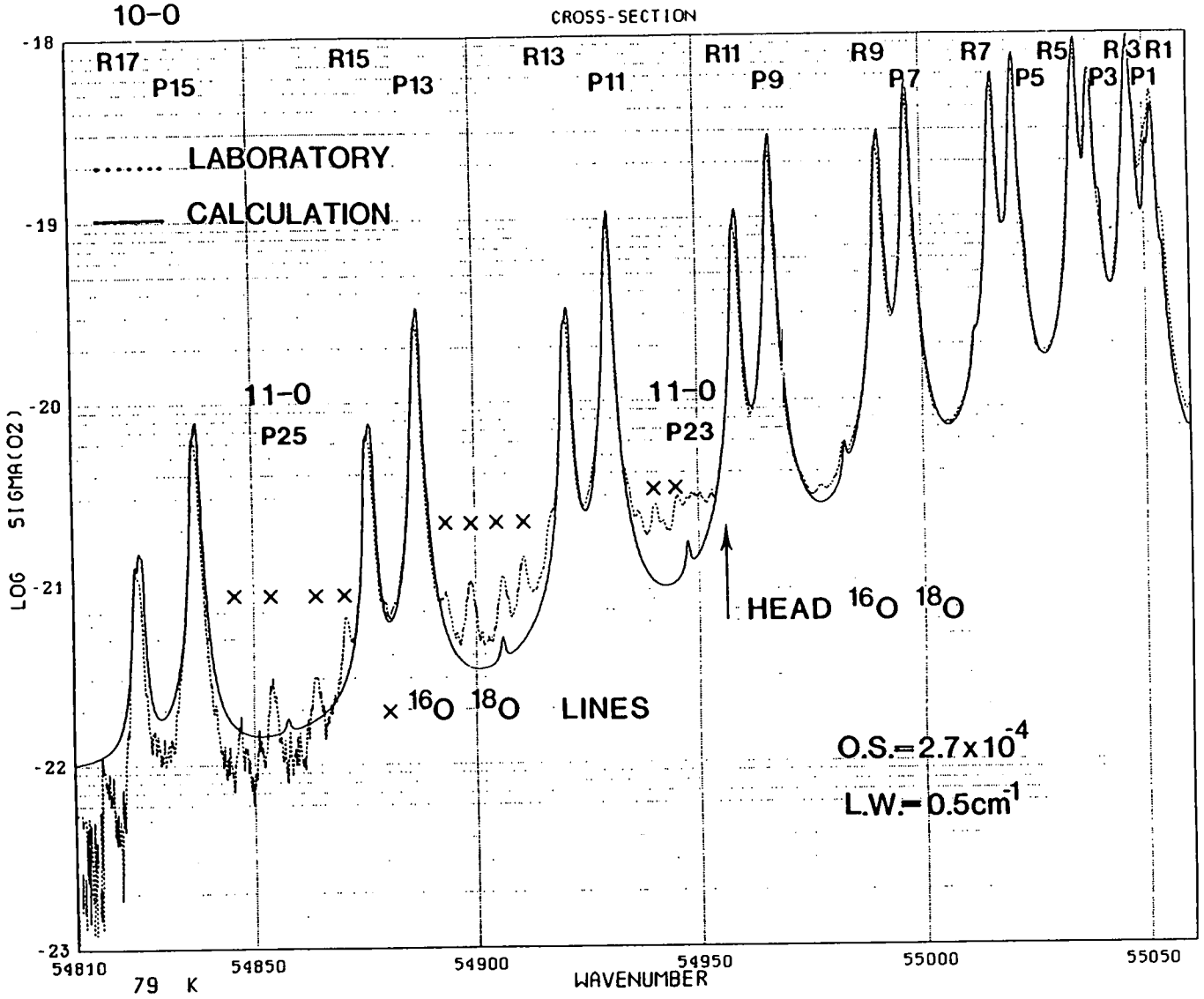

Fig. 12.- Absorption cross sections of the 10-0 band at 79 K.
All aspects described in figures 4 to 10 present in a comparison of theoretical and experimental structures.

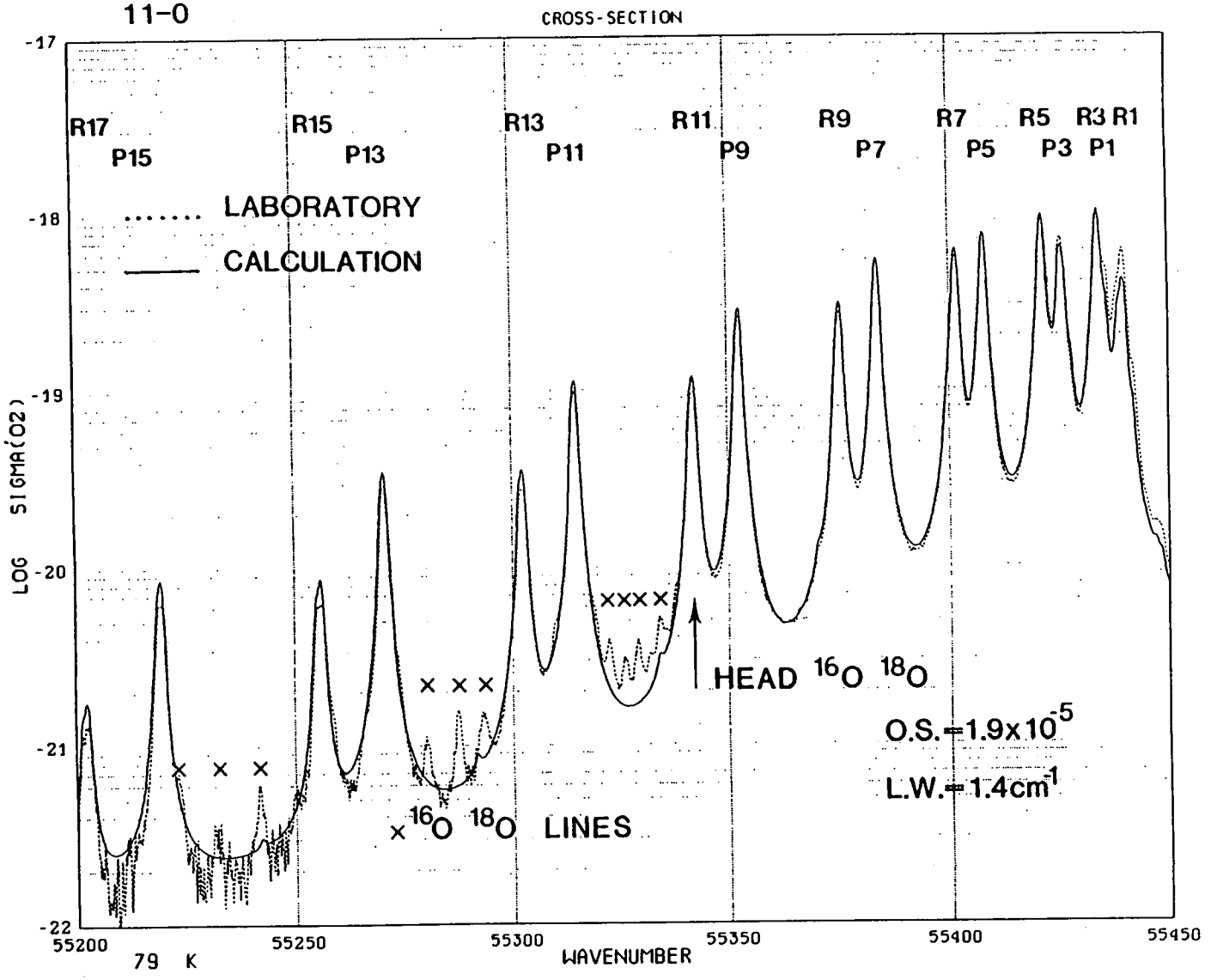

Fig. 13.- Absorption cross sections of the 11-0 band at 79 K. Remarkable differences in structure above and below $^{16}O^{18}O$ head.

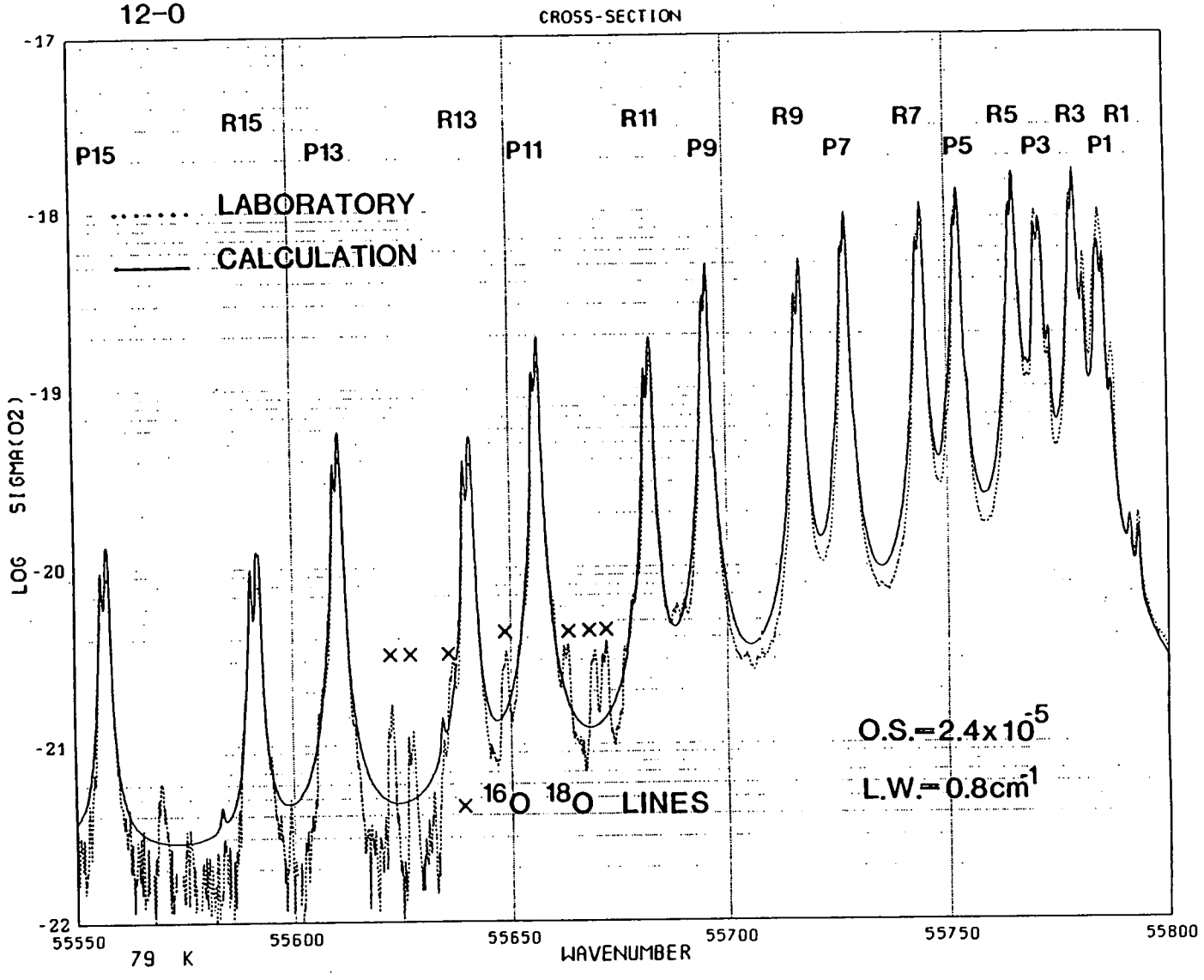

Fig. 14.- Absorption cross sections of the 12-0 band at 79 K. Last band with experimental cross sections.

of the strong noise (logarithmic scale) in the figures corresponding to 2-0 and 3-0 where the continuum cross section is less than 5×10^{-23} cm^2.

Spikes which are clearly apparent in the experimental data, from the 6-0 to 12-0 bands, between the principal lines shown with their assignments are mostly rotational lines of the isotopic molecules ^{16}O ^{18}O. These spectral features are shown in the various figures with an indication of the heads of the $^{16}O^{18}O$ bands. We have verified our assignments thanks to unpublished data (Yoshino-Egmont, personal communication). As an example, the cross sections of the 8-0 bands of $^{16}O_2$ and $^{16}O^{18}O$ are compared in figure 15. It is clear that the four spikes (see Fig. 15) in the window between the P9 and P11 lines of $^{16}O_2$ near 54050 cm^{-1} correspond to the first lines of the $^{16}O^{18}O$ molecules and that the two groups with a double structure between the P11 and P13 lines of $^{16}O_2$ near 54025 cm^{-1} belongs to the $^{16}O^{18}O$ isotopic molecule.

7. COMPARISON BETWEEN THE ABSORPTION STRUCTURES AT 300 K AND 79 K

The theoretical cross sections of the (2-0) to (12-0) bands at 300 K and 79 K have been compared. Two examples are shown in Fig. 16 and 17 for the 2-0 and 4-0 bands. Details of the line assigments (Yoshino et al., 1984; Nicolet et al., 1987) show (see Fig. 1a and 2a, respectively) that the main apparent differences are due to the temperature contrast, specifically the disappearance of the lines corresponding to v" = 1 and the decrease of the intensity of the lines corresponding to v" = 0 at relatively high rotational levels (see Tables 6 and 7). This means that the absorption cross sections at 79 K as shown in Fig. 4 to 14, are practically free from any lines of other bands, and they increase on the lower rotational levels.

8. CONCLUDING REMARK

The high resolution absorption cross sections measurements made by the Harvard-Smithsonian group at 300 K and at 79 K of various bands of the Schumann-Runge system of O_2 have allowed the calculation of line-

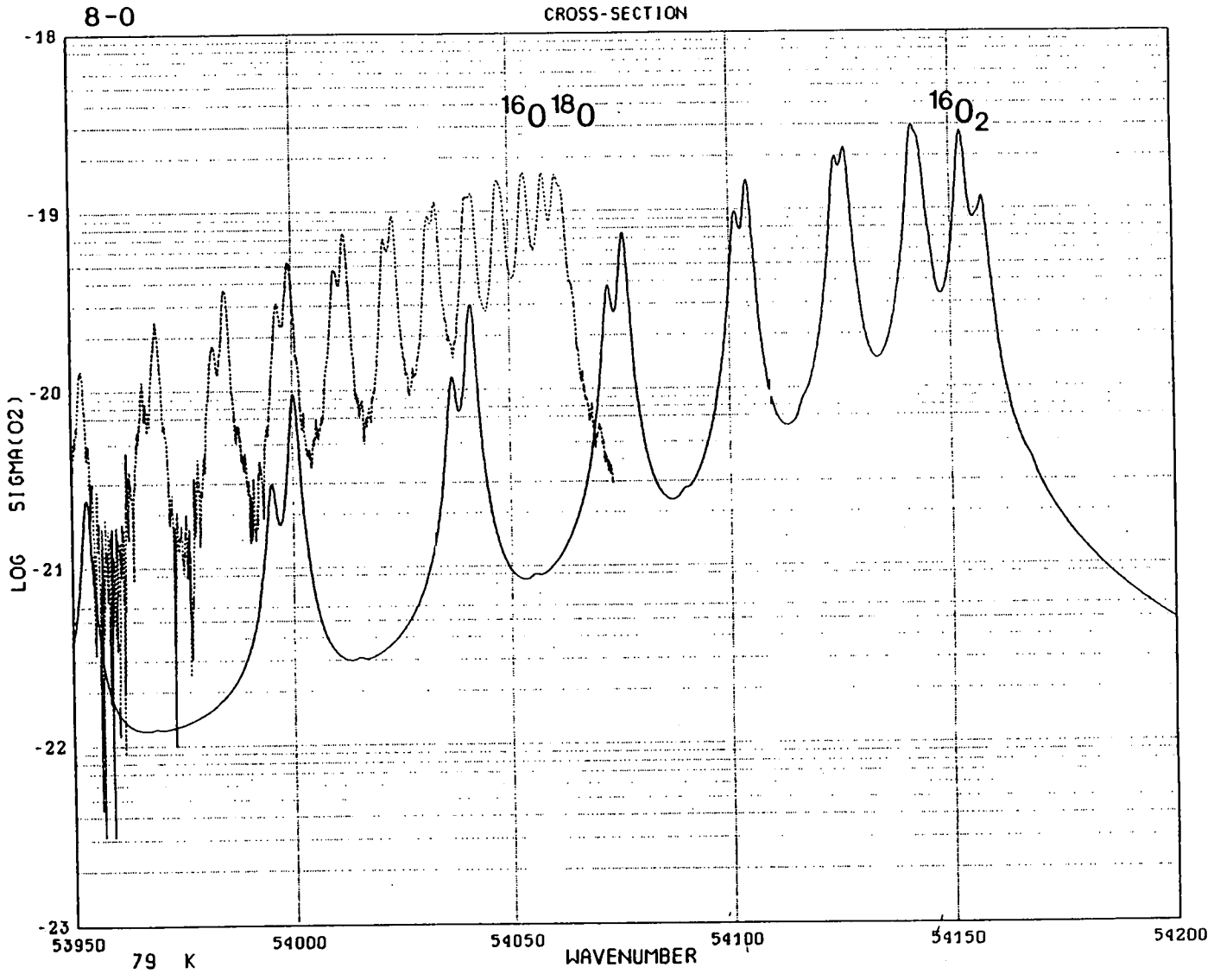

Fig. 15.- Absorption cross sections of the $^{16}O_2$ and $^{16}O^{18}O$ bands at 79 K. Comparison between $^{16}O^{18}O$ experimental and $^{16}O_2$ theoretical determinations.

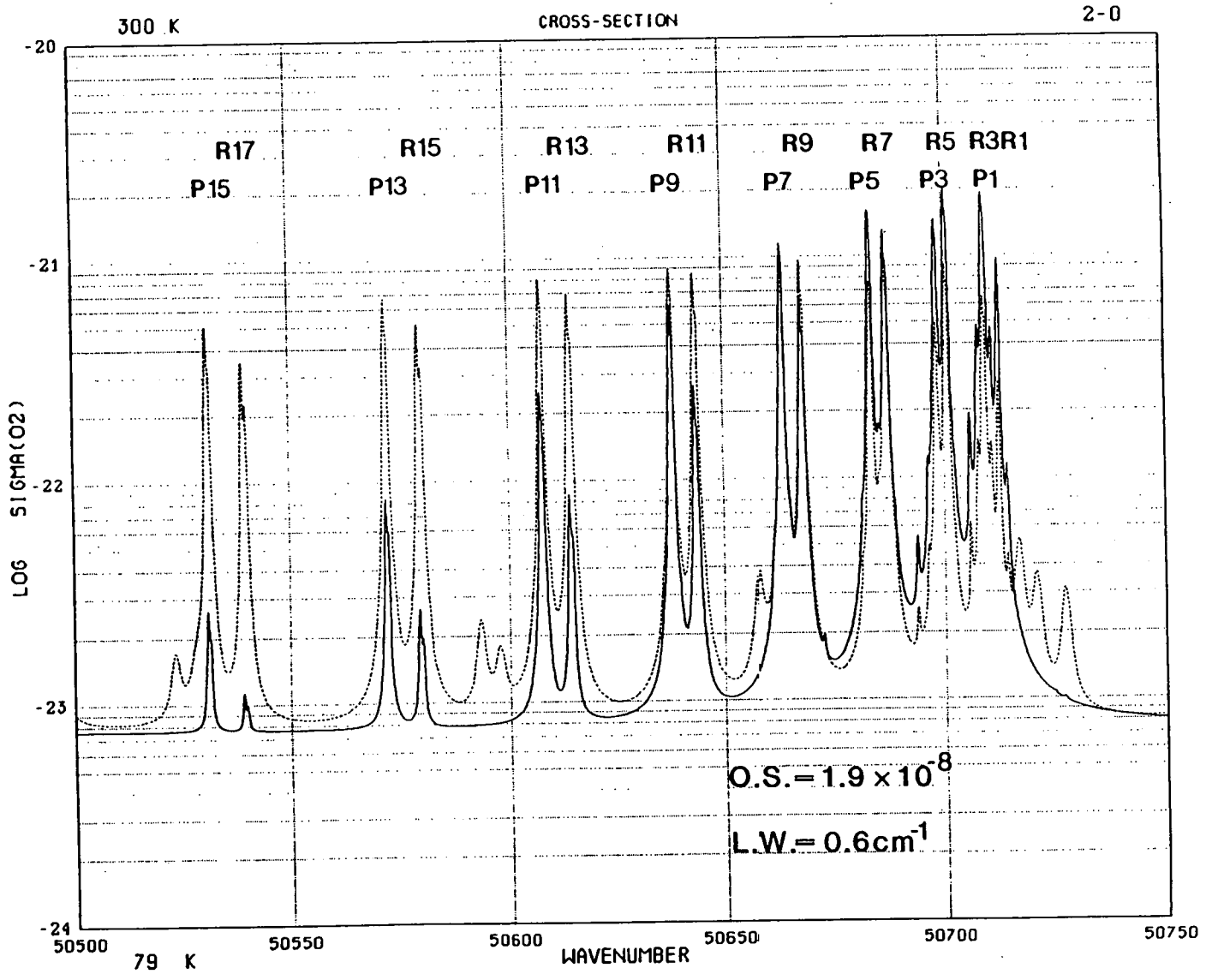

Fig. 16.- Rotational structures of the 2-0 band at 300 K and 79 K.
At high rotation levels, upper curve for 300 K and lower curve for 79 K.
At P7-R9 lines, beginning of an inverted position for both curves.

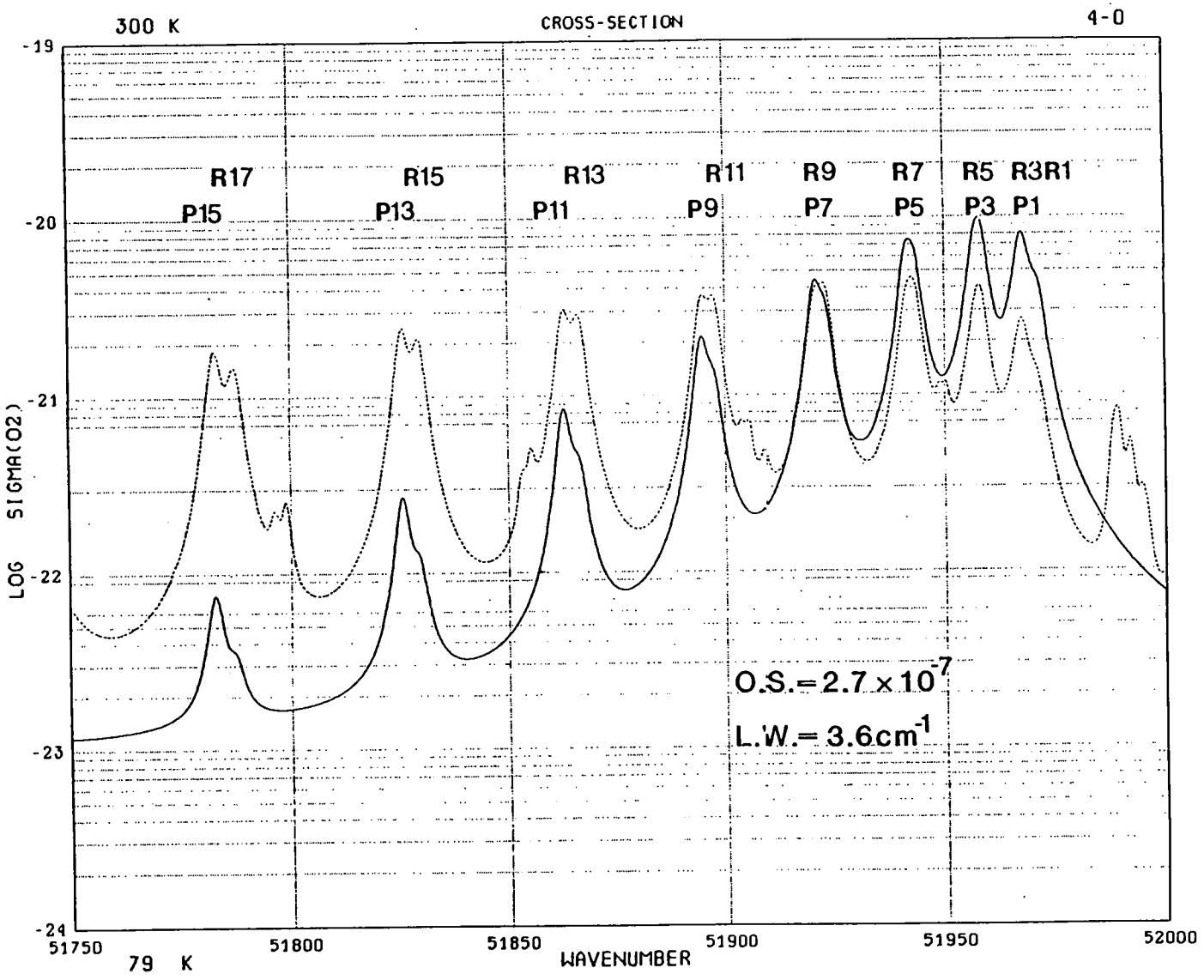

Fig. 17.- Rotational structures of the 4-0 band at 300 K and 79 K.
At high rotation levels, upper curve for 300 K and lower curve for 79 K.
At P7-R9 lines, beginning of an inverted position for both curves.

widths of rotational lines for which the band oscillator strengths were obtained. An accurate calculation of the band structures at various atmospheric temperatures may be performed when adequate averaged linewidths are determined for each band.

ACKNOWLEDGEMENTS

This work is based not only on the most recent publications available, but also on unpublished experimental data. Our special thanks to the members of the Harvard-Smithsonian Group who have kindly provided such data. Support for the preparation of this work has been facilitated by grants of the Commission of the European Communities, Directorate-General for Science, Research and Development, Environment Research Programme, of the Office of Naval Research contract N0014-86-K-0265-P0002 with the Communications and Space Sciences laboratory of Penn state University, and of the Chemical Manufacturers Association Contract FC 85-563 with the Institut d'Aéronomie Spatiale.

REFERENCES

Ackerman, M., and Biaumé, F., Structure of the Schumann-Runge bands from the (0-0) to the (13-0) band, J. Molec. Spectros., 35, 73, 1970.

Allison, A., Dalgarno, A. and Pasachoff, N.W., Absorption by vibrationally-excited molecular oxygen in the Schumann-Runge continuum, Planet. Space Sci., 19, 1463, 1971.

Biaumé, F., Determination de la valeur absolue de l'absorption dans les bandes du Système de Schumann-Runge de l'oxygène moléculaire, Aeronomica Acta, Bruxelles, A, n° 100, 1972.

Brix, P. and Herzberg, G., Fine structure of the Schumann-Runge bands near the convergence limit and the dissociation energy of oxygen molecule, Canad. J. Phys., 32, 110, 1954.

Cheung, A.S.-C., Yoshino, K., Parkinson, W.H. and Freeman, D.E., Herzberg continuum cross section of oxygen in the wavelength region 193.5 - 204.0 nm and band oscillator strength of the (0-0) and (1-0) Schumann-Runge bands, Canad. J. Phys., 62, 1752, 1984.

Cheung, A.S.-C., Yoshino, K., Parkinson W.H. and Freeman, D.E., Molecular spectroscopic constants of O_2 ($^3\Sigma_u^-$), the upper state of the Schumann-Runge bands, J. Molec. spectrosc., 119, 1, 1986.

Fang, T.M., Wofsy, S.C. and Dalgarno, A., Opacity distribution functions and absorption in Schumann-Runge bands of molecular oxygen, Planet. Space Sci., 22, 413, 1974.

Lewis, B.R., Berzins, L., Carver, J.H. and Gibson, S.T., Decomposition of the photoabsorption continuum underlying the Schumann-Runge bands of $^{16}O_2$ - I. Role of the B $^3\Sigma$ state. I - A new dissociation limit, J. Quant. Spectrosc. Rad. Trans., 33, 627, 1985a.

Lewis, B.R., Berzins, L., Carver, J.H., Gibson, S.T. and McCoy, D.G., Decomposition of the photoabsorption continuum underlying the Schumann-Runge bands of $^{16}O_2$. II - Role of the 1 $^3\Pi$ state and collision induced absorption, J. Quant. Spectrosc. Rad. Trans., 34, 405, 1985b.

Lewis, B.R., Berzins, L., Carver, J.H. and Gibson, S.T., Rotational variation of predissociation linewidth in the Schumann- Runge bands of $^{16}O_2$, J. Quant. Spectrosc. Rad. Trans., 36, 187, 1986a.

Lewis, B.R., Berzins, L. and Carver, J.H., Oscillator strengths for the Schumann-Runge bands of $^{16}O_2$, J. Quant. Spectrosc. Rad. Trans., **36**, 209, 1986b.

Nicolet, M., Cieslik, S. and Kennes, R., Rotational structure and absorption cross sections from 300 K to 190 K of the Schumann-Runge bands of O_2, Aeronomica Acta, Brussels, A - n° 318, 1987.

Nicolet, M., and Kennes, R., Aeronomic problems of molecular oxygen photodissociation - I. The O_2 Herzbberg continuum, Planet. Space Sci., **34**, 1043, 1986.

Nicolet, M. and Kennes, R., Aeronomic problems of molecular oxygen photodissociation - IV. The various parameters for the Herzberg continuum, Planet. Space Sci., **36**, 1988.

Yoshino, K., Freeman, D.E., Esmond, J.R. and Parkinson W.H., High resolution absorption cross section measurements and band oscillator strengths of the (1,0) - (12,0) Schumann-Runge bands of O_2, Planet. Space Sci., **31**, 339, 1983.

Yoshino, K., Freeman, D.E. and Parkinson W.H., Atlas of the Schumann-Runge absorption bands of O_2 in the wavelength region 175 - 205 nm, J. Phys. Chem. Ref. Data, **13**, 207, 1984.

Yoshino, K., Freeman, D.E., Esmond, J.R. and Parkinson W.H., High resolution absorption cross sections and band oscillator strengths of the Schumann-Runge bands of oxyge at 79 K, Planet. Space Sci., **35**, 1067, 1987.